UNIVERSIDADE FEDERAL DO PARANÁ

TÁSSIA KARINA WALTER

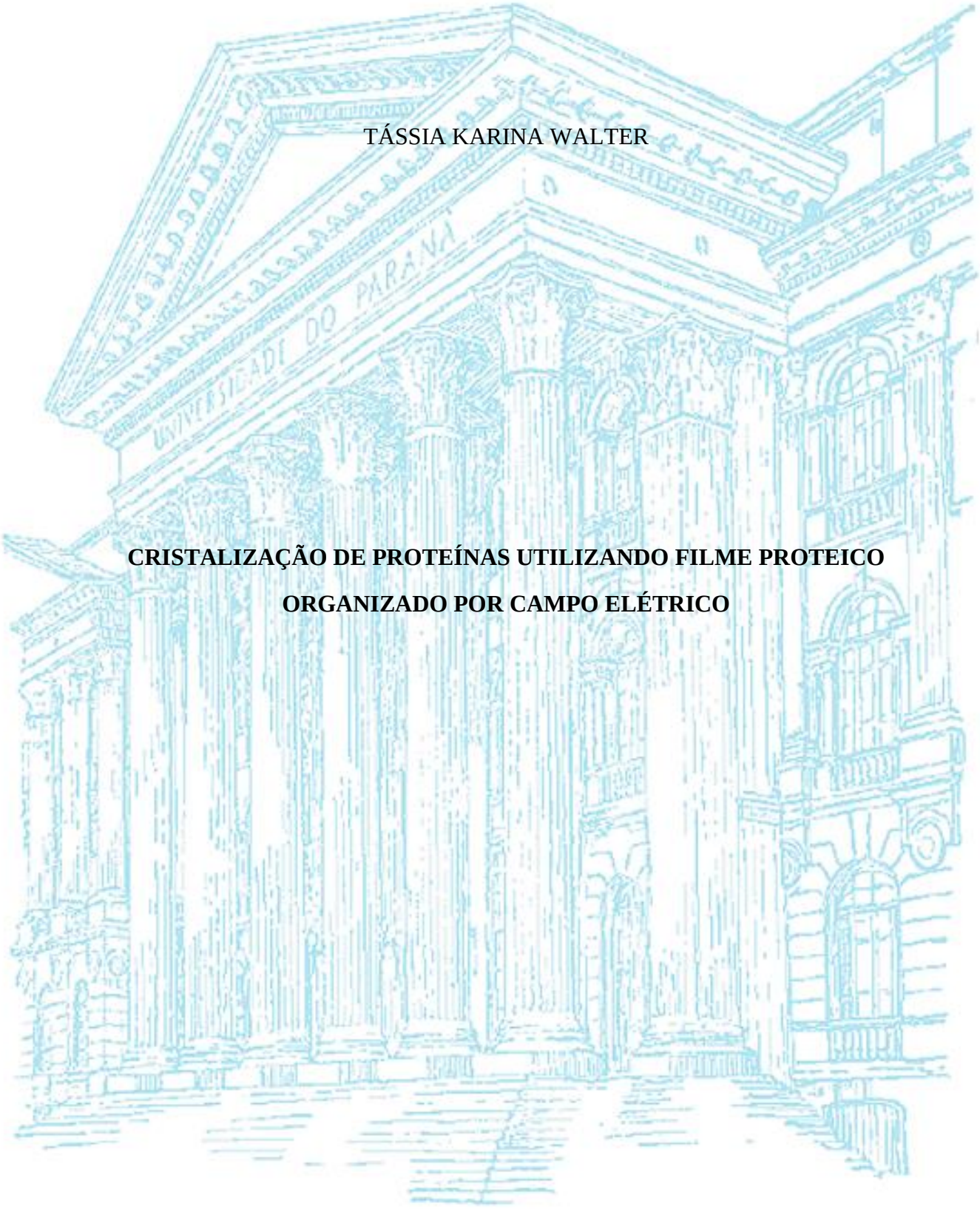

CRISTALIZAÇÃO DE PROTEÍNAS UTILIZANDO FILME PROTEICO ORGANIZADO POR CAMPO ELÉTRICO

CURITIBA
2017

TÁSSIA KARINA WALTER

CRISTALIZAÇÃO DE PROTEÍNAS UTILIZANDO FILME PROTEICO ORGANIZADO POR CAMPO ELÉTRICO

Dissertação apresentada como requisito parcial à obtenção ao grau de Mestre em Bioquímica, no curso de Pós-Graduação em Ciências (Bioquímica), Setor de Ciências Biológicas, Universidade Federal do Paraná.

Orientadora: Prof. Dra. Elaine Machado Benelli.

Co-orientadora: Dra. Cecília Fabiana da Gama Ferreira.

CURITIBA
2017

Universidade Federal do Paraná
Sistema de Bibliotecas

Walter, Tássia Karina
Cristalização de proteínas utilizando filme proteico organizado por campo elétrico. / Tássia Karina Walter. – Curitiba, 2017.
56 f.: il. ; 30cm.

Orientador: Elaine Machado Benelli
Coorientador: Cecília Fabiana da Gama Ferreira

Dissertação (mestrado) - Universidade Federal do Paraná, Setor de Ciências Biológicas. Programa de Pós-Graduação em Bioquímica.

1. Proteinas 2. Cristalização 3. Lisozima I. Título II. Benelli, Elaine Machado III. Ferreira, Cecília Fabiana da Gama Ferreira IV. Universidade Federal do Paraná. Setor de Ciências Biológicas. Programa de Pós-Graduação em Bioquímica.

CDD (20. ed.) 574.19296

MINISTÉRIO DA EDUCAÇÃO

UNIVERSIDADE FEDERAL DO PARANÁ

PRÓ-REITORIA DE PESQUISA E PÓS-GRADUAÇÃO

Setor CIÊNCIAS BIOLÓGICAS

Programa de Pós-Graduação CIÊNCIAS (BIOQUÍMICA)

TERMO DE APROVAÇÃO

Os membros da Banca Examinadora designados pelo Colegiado do Programa de Pós-Graduação em CIÊNCIAS (BIOQUÍMICA) da Universidade Federal do Paraná foram convocados para realizar a arguição da dissertação de Mestrado de **TÁSSIA KARINA WALTER** intitulada **"Cristalização de proteínas utilizando filme proteico organizado por campo elétrico"**, após terem inquerido a aluna e realizado a avaliação do trabalho, são de parecer pela sua aprovação.

Curitiba, 16 de março de 2017.

ELAINE MACHADO BENELLI
Presidente da Banca Examinadora (UFPR)

BEATRIZ GOMES GUIMARAES
Avaliador Interno (UFPR)

RILTON ALVES DE FREITAS
Avaliador Externo (UFPR)

AGRADECIMENTOS

À minha orientadora, prof. Dra. Elaine Benelli, pela orientação, amizade e pelas discussões construtivas que nos levaram a questionamentos e ao aperfeiçoamento do nosso trabalho.

À minha co-orientadora, Dra. Cecília Fabiana Ferreira, por ter compartilhado suas experiências com os filmes de proteína e por estar sempre à disposição para auxiliar com as análises de AFM e FTIR.

À equipe do Laboratório Nacional de Luz Síncrotron, pelo auxílio na coleta de dados de difração de raios-X.

Ao prof. Dr. Jorge Iulek, da UEPG, pelos ensinamentos no processamento de dados de difração de raios-X e pela colaboração no artigo.

Ao Conselho Nacional de Pesquisa (CNPq), pela bolsa de mestrado.

Aos professores a colegas do curso de Pós-Graduação em Ciências (Bioquímica), do Setor de Ciências Biológicas, da UFPR, pelos ensinamentos e troca de experiências.

Aos meus pais, pelo apoio e por sempre acreditarem que a melhor herança é a educação.

“A tarefa não é tanto ver aquilo que ninguém viu, mas pensar o que ninguém ainda pensou sobre aquilo que todo mundo vê.”

(Arthur Schopenhauer)

RESUMO

A análise estrutural de proteínas é uma ferramenta de grande importância na biologia moderna, uma vez que possibilita o estudo do mecanismo de ação de diversas doenças e o desenvolvimento de novos medicamentos. Atualmente, a principal técnica utilizada no estudo da estrutura tridimensional de proteínas é a cristalografia de raios-X, sendo responsável pela resolução de cerca de 90% das estruturas depositadas no Protein Data Bank (PDB). Contudo, a difração de raios-X requer a obtenção de um cristal de proteína de alta qualidade. A cristalização de proteínas é um processo que exige condições específicas, envolvendo uma transição de fase na qual as moléculas de proteína deixam de ser solúveis e passam a formar núcleos organizados. Assim, esse processo é limitado pela nucleação, que requer o choque ordenado das moléculas de proteína para dar início ao crescimento do cristal. Esta, por sua vez, necessita que seja atingida a supersaturação das proteínas em solução. Para atingir essa condição utiliza-se mais comumente a técnica de difusão de vapor, na qual ocorre um aumento de concentração de proteína na gota por meio da difusão lenta de água para um reservatório com maior concentração salina. Quando a condição de supersaturação for atingida muito rapidamente, forma-se um precipitado amorfo em vez de cristais ordenados. Além disso, um nível de saturação muito alto pode levar a formação de inúmeros núcleos, desfavorecendo o crescimento dos cristais e prevalecendo cristais pequenos e de baixa qualidade. Na literatura são propostas diversas alternativas para facilitar a nucleação e crescimento dos cristais, que demandam concentrações menores de proteína e menos tempo. Uma alternativa comum é a chamada nucleação heterogênea, em que o meio cristalizante é semeado com materiais minerais ou orgânicos, como micro-cristais da própria proteína. Outra alternativa é a utilização de um campo elétrico, magnético ou eletromagnético para promover a organização das moléculas na solução de proteína. No entanto, muitas dessas metodologias ainda apresentam limitações, sobretudo com relação a qualidade dos cristais formados. Neste contexto, o presente trabalho apresenta uma nova abordagem para promover a nucleação, empregando a aplicação de um campo elétrico externo durante a formação de um filme protéico e a utilização deste filme organizado como centro de nucleação na cristalização por vapor-difusão. Como modelo de estudo foi utilizada a lisozima de clara de ovo de galinha. Através de imagens de microscopia de força atômica foi possível confirmar a estrutura organizada destes filmes e, por espectroscopia de infra-vermelho por transformada de Fourier foram verificadas pequenas alterações na estrutura secundária da proteína diante da aplicação do campo elétrico. Essa alterações, contudo, não comprometeram a estrutura final da proteína, permitindo um aumento no número de cristais formados, e, em alguns casos, uma melhora da morfologia e aumento do tamanho destes cristais. A análise por difração de raios-X indicou uma melhoria na qualidade da estrutura cristalina, sobretudo em condições nas quais tradicionalmente não se obtêm bons cristais de lisozima.

Palavras-chave: cristalização de proteínas, filme organizado de proteína, lisozima, nucleação.

ABSTRACT

Structural analysis of proteins is a tool of great importance in modern biology, since it allows the study of the mechanism of action of several diseases and the design of new drugs. Nowadays, the main technique used in the study of the three-dimensional structure of proteins is X-ray crystallography, being responsible for the resolution of about 90% of the structures deposited in the Protein Data Bank (PDB). However, X-ray diffraction requires a protein crystal of high quality. The protein crystallization is a process that demands specific conditions involving a transition phase in which protein molecules are no longer soluble and start to form organized nuclei. Thus, this process is limited by nucleation, which requires ordered shock of protein molecules to initiate crystal growth. This, in turn, needs to achieve supersaturation of proteins in solution. In order to reach this condition, the technique of vapor diffusion is used, in which an increase of protein concentration in the drop occurs through the slow diffusion of water to a reservoir with higher salt concentration. When the supersaturation condition is reached very quickly, an amorphous precipitate is formed instead of ordered crystals. In addition, a very high saturation level can lead to the formation of numerous nuclei, disfavoring the growth of crystals and prevailing small and low quality crystals. In the literature, several alternatives are proposed to facilitate nucleation and crystal growth, requiring lower protein concentrations and less time. A common alternative is the so-called heterogeneous nucleation, where the crystallizing medium is seeded with mineral or organic materials, such as microcrystals of the protein itself. Another alternative is the use of an electric, magnetic or electromagnetic field to promote the organization of molecules in the protein solution. However, many of these methods still have limitations, especially regarding to the quality of the crystals formed. In this context, the present work presents a new approach to promote nucleation, employing the application of an external electric field during the formation of a protein film and the use of this organized film as nucleation center in the vapor diffusion crystallization. The chicken egg white lysozyme was used as the study model. Through atomic force microscopy images it was possible to confirm the organized structure of these films, and with Fourier transform infrared spectroscopy were observed small changes in protein secondary structure when the electric field was applied. These changes, however, did not compromise the final structure of the protein, allowing an increase in the number of crystals formed, and, in some cases, an improvement in the morphology and size increase of these crystals. The X-ray diffraction analysis indicated an improvement in the quality of the crystalline structure, especially under conditions in which good crystals of lysozyme are traditionally not obtained.

Keywords: protein crystallization, protein organized film, lysozyme, nucleation.

SUMÁRIO

The use of protein thin film organized by external electric field as template for protein crystallization

Manuscrito formatado para submissão segundo as normas da revista *Crystal Growth & Design* (ISSN 1528-7483)

Fator de impacto 2015: 4.425

THE USE OF PROTEIN THIN FILM ORGANIZED BY EXTERNAL ELECTRIC FIELD AS TEMPLATE FOR PROTEIN CRYSTALLIZATION

[*]Tássia Karina Walter[1], Cecília Fabiana da Gama Ferreira[2], Jorge Iulek[3] and [†]Elaine Machado Benelli[1]

[1]Department of Biochemistry and Molecular Biology, Campus Centro Politécnico, Federal University of Paraná, Av. Coronel Francisco H. dos Santos 100, P.O. Box 19046, 81531-990, Curitiba, Paraná, Brazil.

[2]Department of Engineering, Campus CIC, Faculdade Anchieta de Ensino Superior do Paraná, R. Pedro Gusso 4150, Cidade Industrial, 81315-000, Curitiba, Paraná, Brazil.

[3]Department of Chemistry, State University of Ponta Grossa, Av. Carlos Cavalcanti 4748, 84030-900, Ponta Grossa, Paraná, Brazil.

Corresponding authors: Department of Biochemistry and Molecular Biology, Campus Centro Politécnico, Federal University of Paraná, Av. Coronel Francisco H. dos Santos 100, P.O. Box 19046, 81531-990, Curitiba, Paraná, Brazil. Phone: +55 41 33611653, Fax: +55 41 3266 2042, E-mail: [*]tassiakw@gmail.com, [†]el.benelli@yahoo.com.br.

Abstract

The well-known difficulty to obtain high-quality protein crystals has motivated researchers to come up with new methods or modifications of established crystallization methods to stimulate the growth of good diffracting crystals. In the present work, a new approach, using a protein thin film organized by external electric field (EEF) as template for protein crystal growth, is introduced. This method increased nucleation of hen egg white lysozyme in comparison with the classical vapor diffusion method, besides improving crystal morphology and size. X-ray diffraction analyses indicated improvements in crystal quality. When HEWL was crystallized at pH 6.2, in which this protein presents biological activity, the control crystal presented a poorly ordered crystalline structure and a low resolution cutoff at 3.42 Å, whereas the crystal grown with the EEF protein film revealed a high-resolution limit at 1.67 Å. These results suggest that protein films organized by EEF may improve protein crystals and their data quality.

Keywords: Protein crystallization; Protein thin film; Lysozyme; Template stimulation; Protein nucleation.

1. Introduction

Protein crystallization is a process that requires specific conditions, involving a transition phase in which protein molecules are no longer soluble and form an organized core[1]. In this process, the limiting step is the nucleation[2], which requires not only a supersaturated solution, but also an ordered clustering between protein molecules to initiate crystal growth[3]. In some cases, it is possible to reduce the energy barrier for nucleation by the creation of a microenvironment that favors a higher local concentration of macromolecules[4].

One of the methods used to reduce this energy barrier is heterogeneous nucleation[2]. In this method, nuclei are formed on suspended solid particles or surfaces in contact with the solution. These supports can facilitate the nucleation process by attracting the molecules electrostatically, hydrophobically or through specific interactions, what enables it to occur in metastable conditions[1].

There are several works in the literature that apply heterogeneous nucleation, using distinctive materials as support, such as polymeric films[5], rat whiskers and horse hair[4], bioactive gel-glass particles[2], micromica and natural chlorite[6], self-assembled monolayers[7,8], porous and non-porous microspheres[9]. In the majority of these works, an increase in the crystallization rate, an increase in the size and number of crystals formed and the formation of crystals even under unfavorable conditions could be observed. However, different nucleating materials can affect differently the quality of the crystal formed, due to incompatibilities between their crystal lattices. Occasionally, the binding of crystals to the nucleating agents can also hinder the harvest of single crystals for X-

ray diffraction analyses. Thus, these methods still present limitations, especially with regard to the quality of the crystals formed.

An alternative to promote nucleation and to obtain quality crystals would be to use the protein itself as nucleating centers. In some techniques, small crystals of the protein are used to seed the crystallizing medium and to promote the growth of larger crystals[10]. Nevertheless, dissolution of the seed crystals in medium may happen, and there is the need to produce new seed crystals for each new experiment.

Another way of promoting nucleation and crystal growth is described in works with protein thin films[11–14]. In these studies, protein thin films are formed by the Langmuir-Blodgett (LB) technique, in which the protein solution is applied in a water-air interface followed by immediate submission to high pressure, and then transferred to a glass slide. On this film, a small drop of protein solution is applied and the slide is reversed on the crystallization plate, as in the hanging drop vapor-diffusion method. With this technique, it was possible to obtain micro-crystals of two proteins that, until then, had not been crystallized: bovine cytochrome P450scc and human kinase CKII[12]. In further works with lysozyme, thaumatin, ribonuclease A and proteinase K, analyses revealed that the crystals generated with LB films were larger (about three times) than the crystals without films, using the same solutions, and presented the same resolution (1.6 Å) under X-ray diffraction analyses[15].

At evaluating the effects of synchrotron radiation on crystals formed of LB films, they were found to be more organized, more stable under radiation and with better diffraction limits[13] (when compared with crystals obtained by the classical method), allowing the collection of higher quality data. Moreover, at comparing the electron density maps, structural differences between the models obtained with LB crystals and

classic crystals were observed. Despite of the unique characteristics of LB crystals, some difficulties persist when the method is used for determining the structures of some proteins, especially membrane proteins.

The application of an external electric field (EEF) in the crystallization solution has been extensively studied by several researchers[16–21]. The electric field would have two main effects on a supersaturated solution: molecular orientation and density fluctuation[22]. Density fluctuation occurs mainly due to the electromigration, which leads to an increase in local concentration[23], while the molecular orientation is a result of the molecular polarization, since the electric field creates an oriented dipole, leading to a preferential crystal orientation[24]. The effects of electromigration and molecular orientation caused by an electric field from an alternating current were observed in experiments with lysozyme in solution[18], in which a concentration gradient was established and led to the formation of crystals near the cathode. The EEF application during crystal growth can also improve the crystal quality and extend the resolution, through the increase of the level of crystal internal organization, as verified in another study with lysozyme[20].

The use of an EEF during protein thin film formation was first described in a study with GlnB from *Herbaspirillum seropedicae*[25]. When the electric field was applied the protein molecules were clearly oriented, as observed by atomic force microscopy images[25]. Thus, it is expected that the films formed by the electric field have the potential to act as nucleation centers, what is the starting point for the development of the method proposed on this work.

Therefore, this work attempts to combine the pH variation and the application of an EEF to form an organized protein thin film, which was used as a nucleation center for

protein crystallization. The structure of protein films were analyzed by atomic force microscopy (AFM) and Fourier Transform Infrared spectroscopy (FTIR), and the quality of the crystals was evaluated by X-ray diffraction. We showed that protein thin films organized by EEF can contribute as a nucleation center to protein crystallization.

2. Materials and Methods

2.1. Protein solutions

The classic protein crystallization model, with chicken egg white lysozyme (molecular weight 14300 Da, cat. no. 62970, Sigma-Aldrich Ltd.), was used in our work. Lysozyme is a commercially available protein and has been used as a standard for the development of new methods for protein crystallization. The native protein solution was diluted to a final concentration of 1.43 μg mL^{-1} (100 nM) in 50 mM sodium acetate (pH 4.5) and 50 mM NaCl; in 50 mM MES (2-(N-morpholino)ethanesulfonic acid) (pH 6.2) and 50 mM NaCl; in 50 mM sodium phosphate (pH 6.5) and 50 mM NaCl; and in 50 mM TRIS-HCl (tris(hydroxymethyl)-aminomethane hydrochloride) (pH 8.0) and 50 mM NaCl, to be used for the protein thin film preparation. For crystallization experiments, the protein solution was diluted to 20 $mg.mL^{-1}$ and 40 $mg.mL^{-1}$ in purified water.

2.2. EEF Protein thin film preparation

Each protein solution was dripped on siliconized cover slips (Hampton Research HR 3-231, 22 mm) inside channels (5 mm × 3 mm) made of silicon paste and conductive ink[25]. Each channel was filled with protein solution (20 μL) and then the EEF (300 V, 5 minutes) was applied using a conventional electrophoresis power supply. To determine the best conditions, the current was monitored as described in Ferreira *et al.* (2015). The

same protein solutions were used as control, by simple drop deposition on siliconized cover slips. In addition, solutions prepared with only buffer components were dripped on channels and the same EEF was applied. The films were dried at room temperature.

2.3. Atomic Force Microscopy

Atomic Force Microscopy (Shimadzu SPM9500J3) was used to analyze the topology and phase of protein thin films, as well as of the buffer solutions and controls. The images were obtained in dynamic mode, with a scan rate of 1.3 Hz. A silicon cantilever with spring constant of 36 N/m and radius tip of 10 nm (Nanosensor) was used. The scan direction was aligned with the applied EEF. The measurements were performed at controlled temperature (22 ºC) and humidity (40-50%). In order to eliminate noise and to correct the slope of piezoelectric, the images obtained were treated with Shimadzu software. Three random regions of 10 to 1 μm were chosen in each sample, in order to increase the statistical credibility of results and to describe accurately the structure of the film.

2.4. Fourier Transform Infrared Spectroscopy

In order to verify the structural integrity of the proteins in the film, after the EEF application, Fourier Transform Infrared spectroscopy in Attenuated Total Reflectance mode (FTIR-ATR) was used. Measurements were performed in a Bruker spectrometer

(Vertex 70) with a ZnSe crystal, with the spectrum range between 600 cm^{-1} and 4000 cm^{-1}. All spectra corresponded to an average of 16 scans. The analyses were performed at controlled temperature (20 ºC) and humidity (40%). Spectra of buffer solutions were also obtained, to be compared to the spectra of the protein in the same buffer solutions. After each measurement, the ZnSe crystal was washed with ethanol 70% and purified water. The final spectra are the results of averages of samples in triplicates and measurements in duplicates. All spectra were deconvolved and analyzed with OriginPro 8 software, to identify the position of the main peaks in each condition.

2.5. Crystallization

The protein thin films organized with the EEF were used as templates for crystallization tests. The siliconized cover slips were placed on polyvinyl chloride rings, inside six-well tissue culture plates. With the purpose of determining the composition of reservoir solutions, a classic sitting drop test (without the use of protein thin film as template) was performed. In this test, sodium acetate buffer 50 mM (pH 4.5) with NaCl (500 mM to 1 M) was used as reservoir solution. For comparison, the same conditions were used in crystallization tests with EEF protein thin films. Since in both cases the best crystals were formed at NaCl 780 mM, 900 mM and 1 M, these salt concentrations were also employed in tests with other buffer solutions (at different pHs), especially TRIS-HCl buffer (pH 8.0) and MES buffer (pH 6.2). In each condition, a classic sitting drop test, as well as essays using the protein film with lysozyme in the same reservoir buffer and with lysozyme in phosphate buffer (pH 6.5), was performed, as described by Pechkova & Nicolini[11]. The ratio between the volumes

of the crystallization drop and the reservoir solution was 1:1000. The crystallization experiments were carried out at 20 ºC.

2.6. Data collection and processing

X-ray diffraction data were collected at MX2 beamline of the Brazilian National Synchrotron Laboratory (Campinas, Brazil) [26]. The collection was performed at 100 K, the wavelength was 1.4586 Å and the image exposure times for datasets were between 0.8 and 2.4 s. At least 200 well diffracting images were obtained for each crystal using the PILATUS 2M detector. Crystal to detector distance was 0.100 m in all cases. The cryoprotector used was either 10% glycerol or 15% ethylene glycol, diluted in reservoir solution. The data were integrated, reduced and scaled using XDS and XSCALE. A summary of the data collection statistics is given in Table 2.

3. Results and Discussion

3.1. Atomic Force Microscopy

The lysozyme films formed by drop deposition on siliconized glass slides created clusters, as previously reported in studies of lysozyme adsorption onto mica[27–29]. Kim *et al*. (2002) observed the formation of protein particles on mica surface with height of 2.5 nm and lateral dimensions in the range 10-25 nm, which correspond to a monolayer of lysozyme with approximately five protein molecules per cluster.

In our study, we observed the formation of larger clusters, with sizes that vary according to the pH conditions. In sodium acetate buffer (pH 4.5), mainly supramolecular structures with (60 ± 20) nm (Fig. 1a and 1b) were formed, while in phosphate buffer (pH 6.5), larger structures averaging (500 ± 120) nm (Fig. 1d and 1e) were observed. Yet, in MES buffer (pH 6.2) and in TRIS-HCl buffer (pH 8.0), clusters with (150 ± 50) nm and (250 ± 50) nm of lateral size (Fig. 2a, 2b, 2d and 2e) were present. Since lysozyme presents an ellipsoidal form with dimensions of 3.0 × 3.0 × 4.5 nm[30], the clusters observed can gather tens to hundreds of molecules. Although the protein concentration (1.43 μg mL^{-1}) used was sufficient for a monolayer deposition, the protein diffusion on the surface generated aggregates with one or more protein layers (4-40 nm high).

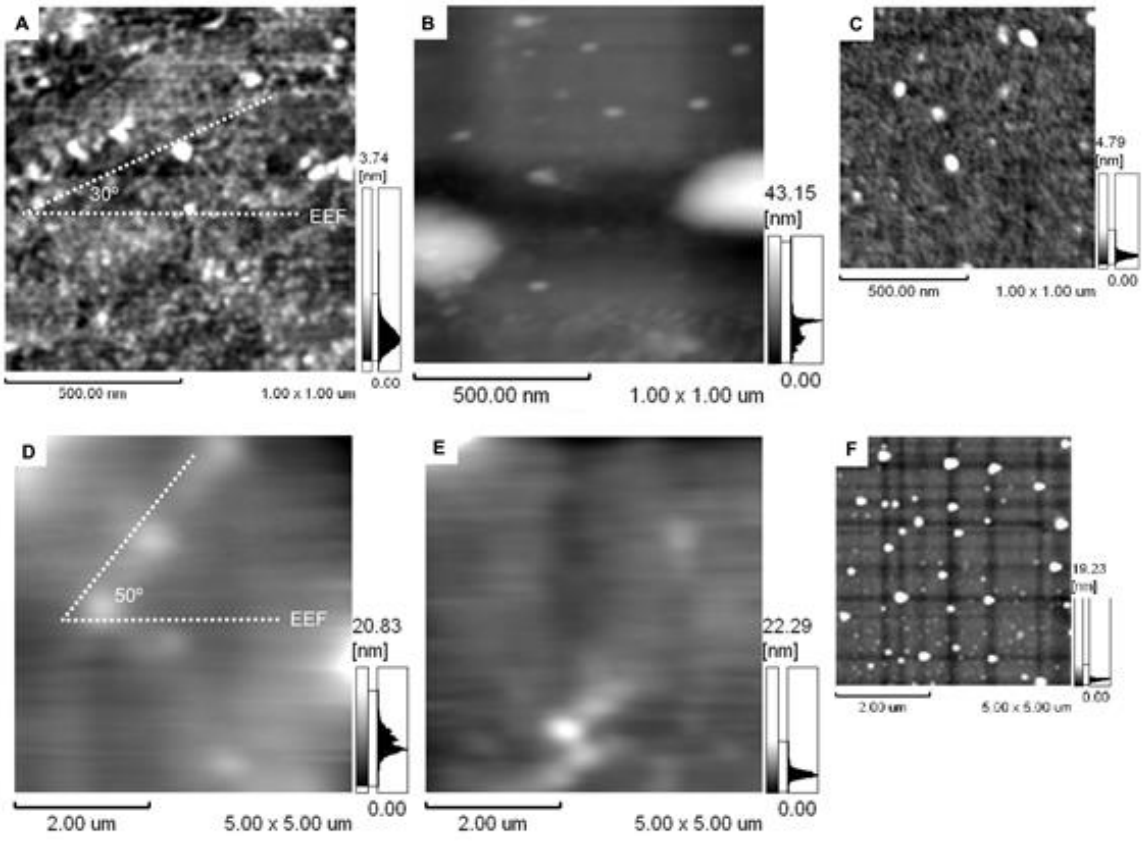

Figure 1. Topographical AFM images of protein films on siliconized glass slides (a) lysozyme in sodium acetate buffer (50 mM, pH 4.5, NaCl 50 mM), with EEF application; (b) in the same solution without EEF application and (c) only sodium acetate buffer solution, exposed to EEF; (d) lysozyme in phosphate buffer (50 mM, pH 6.5, NaCl 50 mM), with EEF application, (e) in same solution without EEF application and (f) only phosphate buffer solution exposed to EEF. The direction of the applied EEF is from left to right.

The application of an EEF during film formation strongly suggests a different distribution of supramolecular structures on the surface, when this is compared to the drop deposition films. As previously reported in a study with GlnB-Hs films[25], the presence of the electric field improves the organization of structures on protein thin films. In sodium acetate buffer (pH 4.5) and in phosphate buffer (pH 6.5), a slight orientation of clusters is seen (Fig. 1a and 1d), at 30º and 50º relative to the direction of electric field application, respectively. Nevertheless, in MES (pH 6.2) and TRIS-HCl

buffers (pH 8.0), a very clear orientation at around 130º and 110º (relative to EEF) can be observed (Fig. 2a and 2d), respectively.

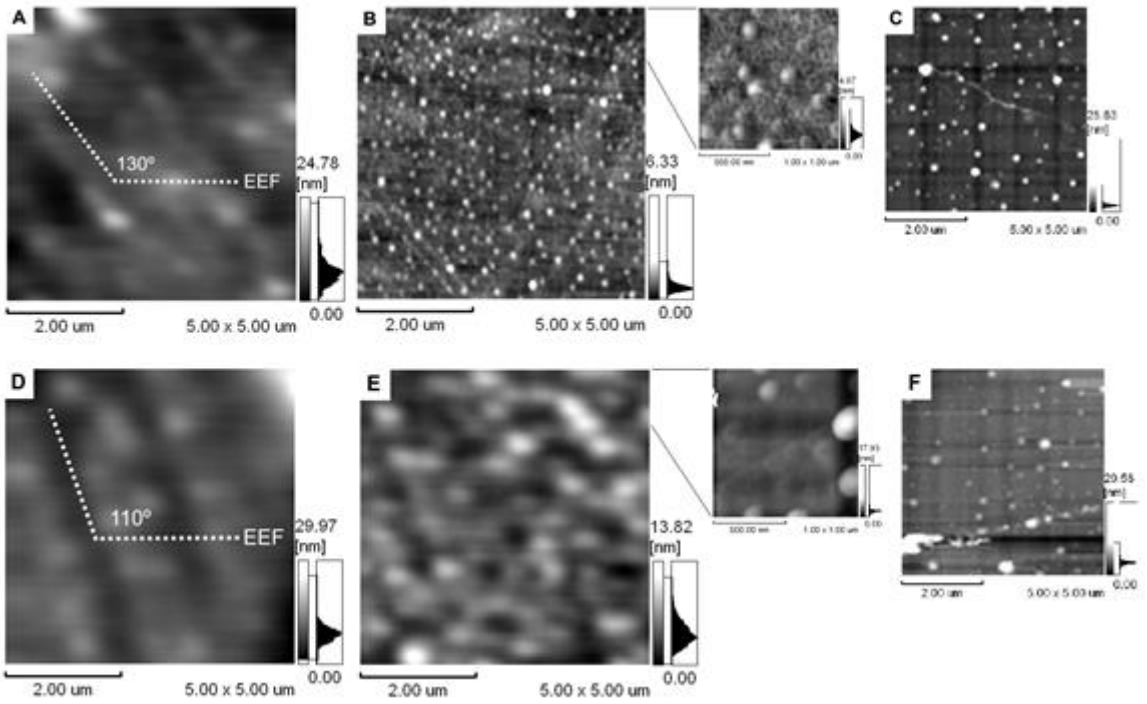

Figure 2. Topographical AFM images of protein films on siliconized glass slides (a) lysozyme in MES buffer (50 mM, pH 6.2, NaCl 50 mM), with EEF application, (b) in same solution without EEF application and (c) only MES buffer solution exposed to EEF; (d) lysozyme in TRIS-HCl buffer (50 mM, pH 8.0, NaCl 50 mM), with EEF application, (e) in same solution without EEF application and (f) only TRIS-HCl buffer solution exposed to EEF. The direction of the applied EEF is from left to right.

On the other hand, the drop deposition films presented a sparse distribution of supramolecular structures throughout the surface, leading to formation of large clusters (Fig. 1b and 1e) or having better area coverage (Fig. 2b and 2e).

Once the buffer compounds form similar structures in drop deposition films[25,31], AFM images have been taken from thin films formed by buffer solution exposed to EEF. These images showed no evidence of orientation and a random distribution of

buffer compounds (Fig. 1c, 1f, 2c and 2f), similar to the pattern seen in the drop deposition protein films. Thus, the orientation would be related to the presence of large polar molecules, like proteins[25], but not to buffer compounds. Despite this, the buffer composition directly interferes in the distribution profile of structures on protein thin films, when exposed to electric field, as can be seen in Fig. 1a, 1d, 2a and 2d.

3.2. Fourier Transform Infrared Spectroscopy

The final averaged FTIR spectrum of lysozyme films for each buffer condition is shown in Fig. S1. Although a spectrum range between 600 cm^{-1} and 4000 cm^{-1} was used in the measurements, the amide I band, from 1600 cm^{-1} to 1700 cm^{-1}, was used to analyze the results. This band corresponds to the vibration mode mostly used in studies of protein secondary structure and originates mainly from C=O stretching of the amide group[32]. The Gaussian peak fitting procedure has been applied to the averaged FTIR spectra (OriginPro 8 software). To optimize the fit, eight Gaussian fitting curves were used for spectral deconvolution. The quality of the fitting was evaluated on the basis of χ^2 values (on the order of 10^{-7}) and correlation coefficient values ($\geq$ 0,999).

Hen egg white lysozyme structure is composed of six α-helices and three β-sheets connected by few flexible loops[29]. In solution, lysozyme exhibits an amide I maximum at 1654 cm^{-1}, typical of a protein with predominant α-helix secondary structure, and minor absorptions at 1630 and 1673 cm^{-1} (corresponding to extended chains like in the β-sheet structure), 1641 cm^{-1} (unordered structures), 1666 and 1682 cm^{-1} (turns and bends)[33]. However, as hydrated film on an attenuated total reflectance (ATR) plate, lysozyme presents different frequency absorption, the maxima at 1646 and 1654 cm^{-1}

(α-helix), 1630 cm^{-1} (β-sheet), and minor frequency absorptions at 1638 and 1662 cm^{-1} (random coil), 1670 and 1678 cm^{-1} (β-turns)[34].

Comparing the FTIR spectra of lysozyme films formed by drop deposition (control) with the spectra of lysozyme films formed by EEF application, it was possible to observe a shift in the α-helix frequency, especially in the spectra of the protein in sodium acetate buffer and in TRIS-HCl buffer (Fig. S1). In Table 1, the deconvolved frequencies are summarized and it is possible to observe a shift from 1661 cm^{-1} to 1657 cm^{-1}, when the protein is in sodium acetate buffer, and from 1659 cm^{-1} to 1656 cm^{-1}, when the protein is in TRIS-HCl buffer. This difference could be attributed to structural rearrangements of the protein[32]. The shift in the α-helix frequency was also observed in lysozyme Langmuir-Schaefer films when treated at high temperatures[35], what is attributed to the stabilization of the helical structure upon removal of water molecules. The difference in the distribution of particles on the films may actually interfere with water adsorption, which also leads to a difference in the signal observed in the spectra of the control and the EEF films.

Concerning the β-sheet frequency, it was possible to verify a shift to a lower wavenumber in the spectra of the protein in MES and in phosphate buffers, from 1639 cm^{-1} to 1633 cm^{-1} and from 1640 cm^{-1} to 1631 cm^{-1}, respectively. Furthermore, the region corresponding to antiparallel β-sheets or turns also presents a shift in the peaks. While absorptions at 1682-1684 cm^{-1} can be assigned in control films, the EEF films present absorptions at 1677-1680 cm^{-1} and 1690-1694 cm^{-1}. Once more, we can infer a structure reorganization of the protein after EEF application.

Table 1 – Deconvolved amide I frequencies (cm^{-1}) for lysozyme films

	Lysozyme films formed with drop deposition (control)				**Lysozyme films formed with EEF**			
Buffer solution	*Acetate (pH 4.5)*	*MES (pH 6.2)*	*Phosphate (pH 6.5)*	*TRIS-HCl (pH 8.0)*	*Acetate (pH 4.5)*	*MES (pH 6.2)*	*Phosphate (pH 6.5)*	*TRIS-HCl (pH 8.0)*
Aggregated (1610-1628)*	1619	1621	1621	1619	1626	1625	1619	1621
β-sheet (1625-1640)*	1629	1639	1640	1633	1632	1633	1631	1631
Random coil (1640-1648)*	1640	-	-	1644	1644	1643	-	1643
α-helix (1648-1660)*	1651	1650 1656	1650 1658	1651 1659	1651 1657	1650 1657	1650	1650 1656
3_{10}-helix (1660-1670)*	1661 1666	1664	1670	1667	1664	1666	1661 1669	1665
Antiparallel β-sheet/ turns (1675-1695)*	1684	1684	1684	1675 1682	1677 1691	1678 1690	1680 1694	1678 1690

*According to Jackson & Mantsch (1995) [32]

3.3. Crystallization under different conditions

The crystallization tests were performed at three different pH: acid, employing sodium acetate (pH 4.5) as buffer, which is the most widely used pH for lysozyme crystallization; alkaline, using TRIS-HCl (pH 8.0) as buffer; and the pH of lysozyme biological activity (pH 6.2), for which MES buffer was used.

In sodium acetate buffer, as expected, there were no difficulties for crystal appearance in a few days, even without the use of the protein film (Fig. 3a, 3d). However, the use of the EEF film as template allowed the formation of a higher number of crystals, clearly due to an increase in nucleation (Fig. 3b, 3c). At conditions with lower salt concentration, in which there was precipitation in the control assays, the film allowed the growth of large and regular crystals. In some cases, the use of the film

retarded the emergence of crystals, however, it contributed to the formation of larger and symmetrical crystals (Fig. 3e, 3f), what can be important for improving data collected by X-ray diffraction.

Nevertheless, at the pH condition in which the enzyme presents biological activity (MES buffer, pH 6.2), the control tests required more time (about one month) to crystallize and, moreover, only a few small crystals were formed (Fig. 3g). Only at higher protein concentration, larger crystals could be obtained (Fig. 3j). On the other hand, with the use of the EEF protein films, the time for crystal emergence was reduced to one week. In addition, nucleation was stimulated once again (Fig. 3h, 3i), leading to the generation of several medium-size crystals. Although the growth of larger crystals took longer time (two to six months), the method of EEF protein film produced regular crystals (Fig. 3k, 3l).

Under alkaline conditions (TRIS-HCl buffer, pH 8.0), a large number of small crystals appeared in the control tests, when lower protein concentration was used (Fig. 3m). When a higher protein concentration was employed, either precipitation occurred (in some conditions) or crystals with an irregular shape were formed (Fig. 3p). In contrast, the EEF protein films enabled the growth of larger and more symmetrical crystals (Fig. 3q, 3r) in shorter time. Even at low protein concentrations, when the nucleation is favored, crystals of medium size were observed (Fig. 3n, 3o).

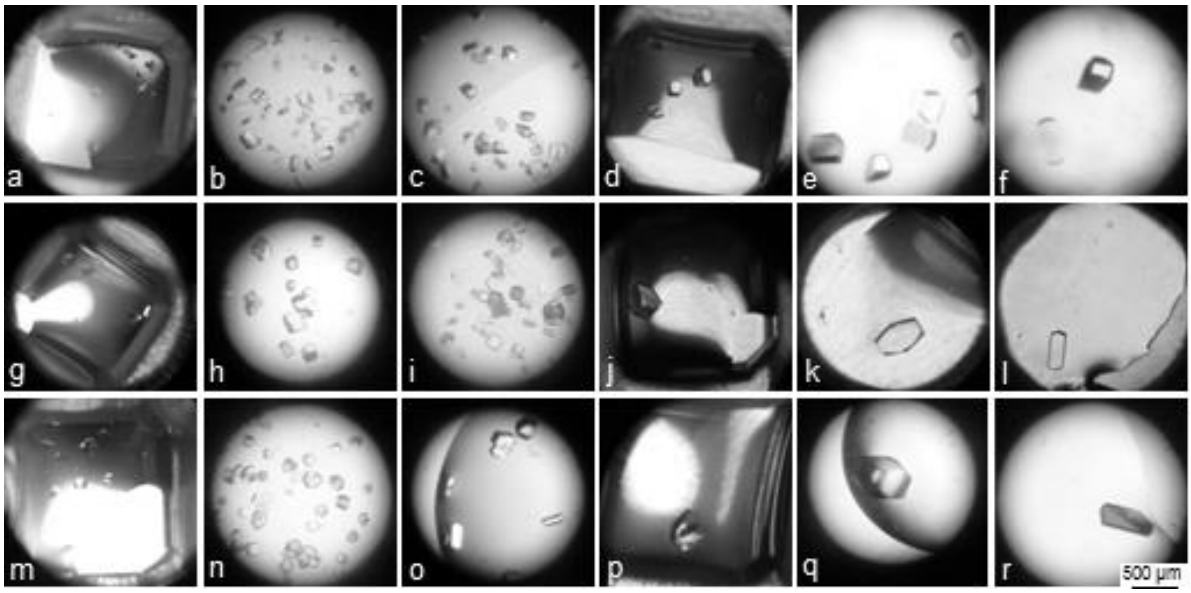

Figure 3. Lysozyme **c**rystals obtained by classical vapor-diffusion method without the use of protein thin films (controls) (a, d, g, j, m, p) and using EEF protein thin films in phosphate buffer (b, e, h, k, n, q), in sodium acetate buffer (c, f), in MES buffer (i, l) and in TRIS-HCl buffer (o, r). Reservoir solution: sodium acetate buffer 50 mM (pH 4.5) with 1 M NaCl (a), 780 mM NaCl (b, c, d, f) and 900 mM NaCl (e); MES buffer 50 mM (pH 6.2) with 1 M NaCl (g, j, k), 780 mM NaCl (h, i) and 900 mM NaCl (l); TRIS-HCl buffer 50 mM (pH 8.0) with 780 mM NaCl (m), 900 mM NaCl (n, p, q, r) and 1 M NaCl (o). Drop solution: 1:1, lysozyme 10 $mg.mL^{-1}$ (a, b, c, g, h, i, m, n, o) and 20 $mg.mL^{-1}$(d, e, f, j, k, l, p, q, r).

In addition, tests were performed with standard crystallization solutions (Hampton Research Crystal Screens, HR2-110 and HR2-112). Six solutions of different pH from each crystallization kit were chosen. In some conditions, crystal formation was observed only when the EEF protein film was used as template, namely: 100 mM imidazole (pH 6.5) with 1 M sodium acetate; 100 mM HEPES (pH 7.5) with 100 mM NaCl and 1.6 M ammonium sulfate; and 100 mM sodium cacodylate (pH 6.5) with 200 mM magnesium acetate and 20% polyethylene glycol 8000. In other cases, such as in 100 mM MES (pH 6.5) with 200 mM ammonium sulfate and 30% polyethylene glycol monomethyl ether 5000, it was possible to observe an increase in the number of crystals formed.

Our results agree with studies in that usage of Langmuir-Blodgett protein thin films led to a positive influence in protein nucleation, with an acceleration of crystal growth

rate, in comparison with the classical hanging drop method[11,12]. In addition, the crystals obtained with LB films are larger than those grown with classical method[11,15], what was also observed in our study.

3.4. Diffraction quality analyses of lysozyme crystals

The quality of lysozyme crystals grown under different conditions was analyzed by X-ray diffraction. For these experiments, crystals with good morphology and similar size for each pH condition were selected, such that more than one crystal from each situation was used. Table 2 summarizes the diffraction data statistics for crystals grown with and without the use of EEF protein thin film as template, obtained after data processing with XDS and XSCALE.

In order to compare the quality of crystals, three concomitant criteria were used to determine the diffraction resolution limit: global completeness ≥ 95%, $\langle I/\sigma(I)\rangle \geq 1.0$ and $CC_{1/2} \geq 50\%$ on the highest resolution shell. Recent studies have shown that, in some cases, there is useful information remaining even when $CC_{1/2}$ falls to around 40 – 20% and $\langle I/\sigma(I)\rangle$ to around 1.5 – 0.5 [36], for model improvement. Despite being widely used for determining the resolution cutoff, R_{meas} or R_{merge} values should play no role to define the high-resolution limit, since they can discard many useful data[37,38].

The diffraction analyses indicated that crystals formed in sodium acetate buffer without protein film presented the highest resolution limit. This was already expected, since it is the most widely used condition for lysozyme crystallization. Nevertheless, the EEF crystal in phosphate buffer (crystal A2) also exhibited a good resolution limit. The lower resolution limit presented by the EEF crystal in sodium acetate buffer (crystal A1)

could be related to the small conformational changes observed by FTIR analyses, which affect the crystalline structure and increase the crystal mosaicity, as can be seen in Table 2.

Table 2 –X-ray diffraction data statistics of lysozyme crystals grown with and without EEF protein thin film

	Lysozyme crystallized in sodium acetate buffer (pH 4.5)			**Lysozyme crystallized in MES buffer (pH 6.2)**			**Lysozyme crystallized in TRIS-HCl buffer (pH 8,0)**		
	Control	**Crystal A1***	**Crystal A2****	**Control**	**Crystal M1***	**Crystal M2****	**Control**	**Crystal T1***	**Crystal T2****
Space group	$P4_32_12$	$P4_32_12$	$P4_32_12$	$P4_32_12$	$P4_32_12$	$P4_32_12$	$P4_32_12$	$P4_32_12$	$P4_32_12$
Unit cell (Å)	a= 78.25 b= 78.25 c= 36.62	a= 78.25 b= 78.25 c= 36.62	a= 78.25 b= 78.25 c= 36.62	a= 77.29 b= 77.29 c= 36.71	a= 78.25 b= 78.25 c= 36.62	a= 78.25 b= 78.25 c= 36.62	a= 78.25 b= 78.25 c= 36.62	a= 78.25 b= 78.25 c= 36.62	a= 78.25 b= 78.25 c= 36.62
Total reflections	95608 (1604)	60581 (5182)	82883 (2966)	10015 (1056)	73719 (2557)	85196 (3006)	93631 (1691)	50564 (1798)	83139 (2985)
Unique reflections	18053 (874)	9074 (770)	13402 (664)	1632 (180)	11423 (540)	13679 (687)	17206 (623)	13047 (587)	13449 (643)
Multiplicity	5.30 (1.84)	6.68 (6.73)	6.18 (4.47)	6.14 (5.87)	6.45 (4.74)	6.23 (4.38)	5.44 (2.71)	3.87 (3.06)	6.18 (4.64)
Resolution range (Å)	78 - 1.51 (1.54 - 1.51)	78 - 1.92 (1.98 - 1.92)	78 - 1.68 (1.71 - 1.68)	78 - 3.42 (3.56 - 3.42)	78 - 1.77 (1.80 - 1.77)	78 - 1.67 (1.70 - 1.67)	78 - 1.52 (1.55 - 1.52)	78 - 1.67 (1.70 - 1.67)	78 - 1.67 (1.70 - 1.67)
Completeness (%)	98.1 (85.2)	99.5 (99.6)	99.5 (99.3)	96.5 (98.4)	98.8 (98.7)	99.8 (98.7)	95.3 (62.2)	95.2 (84.3)	98.1 (92.4)
R_{meas} *(%)*	5.9 (67.6)	17.5 (187.1)	10.4 (132.6)	41.0 (48.6)	11.7 (110.7)	8.2 (121.9)	4.5 (12.0)	3.2 (15.5)	7.9 (51.1)
I/σ(I)	15.00 (1.04)	8.02 (1.09)	11.91 (1.38)	2.98 (2.79)	10.67 (1.67)	15.09 (1.43)	24.28 (8.05)	29.85 (8.25)	14.40 (3.24)
$CC_{1/2}$	99.9 (59.1)	99.4 (57.2)	99.8 (51.5)	94.6 (92.8)	99.7 (53.5)	99.9 (51.5)	99.9 (97.8)	99.9 (97.3)	99.7 (86.3)
Mosaicity	0.29518	0.58000	0.30339	0.58234	0.25500	0.23221	0.27367	0.24687	0.28607

* using as template for crystal growth a film of lysozyme in crystallization buffer.

** using as template for crystal growth a film of lysozyme in phosphate buffer.

The lysozyme crystals obtained using Langmuir-Blodgett films at the same buffer conditions was reported to show a high-resolution limit, at 1.57 Å, with $\langle I/\sigma(I)\rangle$ of 0.1 and completeness of 26.83%[14]. Despite the resolution cut-off criteria for LB crystals

were different from ours, we can say that our method propitiated also a high-resolution for EEF crystals in phosphate buffer, at 1.68 Å, with better diffraction quality ($\langle I/\sigma(I)\rangle$ of 1.38 and completeness of 99.3%).

In alkaline conditions, where TRIS-HCl buffer was used for crystallization, crystals obtained with EEF protein film demonstrated diffraction properties similar to control crystal, despite presenting slightly lower resolution limits. Interestingly, in this pH condition, the space group and the unit cell dimensions are exactly the same for the crystal in sodium acetate buffer. This fact may be related to the remarkable structural stability of lysozyme in different pH conditions[39].

On the other hand, when MES buffer (pH condition of lysozyme biological activity) was used, EEF protein films led to a dramatic improvement in the diffraction properties of lysozyme crystals. The control crystal showed a less ordered crystalline structure, partly due to high mosaicity, resulting in lower diffraction power and resolution limit. Compared to the control, the resolution limit increased from 3.42 Å to 1.67 Å (with EEF film in phosphate buffer). In contrast to what occurred in sodium acetate buffer, the EEF protein film in MES and in phosphate buffer has apparently improved the crystalline structure of lysozyme crystals, allowing the better resolutions achieved by X-ray diffraction.

4. Conclusions

In this work, lysozyme crystallization was investigated using as nucleation center a protein thin film obtained with the application of an EEF. Different pH conditions were assayed, not only during the protein film preparation, but also in the crystallization tests. Regarding to the lysozyme films, AFM images have suggested an orientation of structures when EEF was applied, especially in the ones where MES and TRIS-HCl buffer were used. The FTIR spectra of lysozyme films demonstrated some small frequency shifts, indicating possible structural rearrangements of the protein in the EEF films.

Despite this, the organized structure of the EEF protein film has increased nucleation in all tested conditions, leading to the formation of a larger number of crystals and, sometimes, also contributing to the improvement of their size and/or morphology. Diffraction analyses of the crystals grown with EEF protein films revealed a significant improvement of the diffraction properties of the ones obtained at pH 6.2, which corresponds to the biological activity of lysozyme.

The results suggest that the EEF protein films could be particularly useful for the crystallization of proteins at lower initial concentration, thus using small protein amounts and not requiring crystallization kits to obtain crystals. Furthermore, this new approach opens possibilities to study a protein structure in its physiological condition, what may bring insights regarding its active structure. This method is easily performed in any laboratory.

Further work is necessary to understand the mechanisms of EEF protein thin film influence in protein crystallization and nucleation. Of remarkable importance, it would

be to continue the investigation with other protein models, in order to verify if these achievements are reproducible.

Conflict of Interest

The authors have no conflict of interest in this work.

Supplementary material

Figure S4. FTIR average spectra of lysozyme thin films formed by drop deposition and by EEF application.

Acknowledgments

T. K. Walter would like to thank CNPq (Conselho Nacional de Pesquisa) for the MSc Scholarship, the Brazilian National Synchrotron Laboratory (Campinas, Brazil) for the beamline use and the Nitrogen Fixation Laboratory (UFPR) for equipment use.

References

(1) Bolanos-Garcia, V. M.; Chayen, N. E. *Prog. Biophys. Mol. Biol.* **2009**, *101* (1–3), 3.

(2) Chayen, N.; Saridakis, E.; Sear, R. *Proc. Natl. Acad. Sci. U. S. A.* **2006**, *103* (3), 597.

(3) Vekilov, P. G. *Cryst. Growth Des.* **2010**, *10* (12), 5007.

(4) D'Arcy, A.; Mac Sweeney, A.; Haber, A. *Acta Crystallogr. - Sect. D Biol. Crystallogr.* **2003**, *59* (7), 1343.

(5) Fermani, S.; Falini, G.; Minnucci, M.; Ripamonti, A. *J. Cryst. Growth* **2001**, *224* (3–4), 327.

(6) Takehara, M.; Ino, K.; Takakusagi, Y.; Oshikane, H.; Nureki, O.; Ebina, T.; Mizukami, F.; Sakaguchi, K. *Anal. Biochem.* **2008**, *373* (2), 322.

(7) Pham, T.; Lai, D.; Ji, D.; Tuntiwechapikul, W.; Friedman, J. M.; Lee, T. R. *Colloids Surfaces B Biointerfaces* **2004**, *34* (3), 191.

(8) Zhang, C. Y.; Shen, H. F.; Wang, Q. J.; Guo, Y. Z.; He, J.; Cao, H. L.; Liu, Y. M.; Shang, P.; Yin, D. C. *Int. J. Mol. Sci.* **2013**, *14* (6), 12329.

(9) Guo, Y.-Z.; Sun, L.-H.; Oberthuer, D.; Zhang, C.-Y.; Shi, J.-Y.; Di, J.-L.; Zhang, B.-L.; Cao, H.-L.; Liu, Y.-M.; Li, J.; Wang, Q.; Huang, H.-H.; Liu, J.; Schulz, J.-M.; Zhang, Q.-Y.; Zhao, J.-L.; Betzel, C.; He, J.-H.; Yin, D.-C. *Sci. Rep.* **2014**, *4*, 7308.

(10) D'Arcy, A.; Sweeney, A. Mac; Haber, A. *J. Synchrotron Radiat.* **2004**, *11* (1), 24.

(11) Pechkova, E.; Nicolini, C. *J. Cryst. Growth* **2001**, *231* (4), 599.

(12) Pechkova, E.; Nicolini, C. *J. Cell. Biochem.* **2002**, *85* (2), 243.

(13) Pechkova, E.; Nicolini, C. *Anticancer Res.* **2010**, *30* (7), 2745.

(14) Nicolini, C.; Belmonte, L.; Riekel, C.; Koenig, C.; Pechkova, E. *Am. J. Biochem. Biotechnol.* **2014**, *10* (1), 22.

(15) Pechkova, E. *J. Nanomed. Nanotechnol.* **2014**, *5* (6).

(16) Hammadi, Z.; Astier, J. P.; Morin, R.; Veesler, S. *Cryst. Growth Des.* **2007**, *8*, 1476.

(17) Revalor, E.; Hammadi, Z.; Astier, J. P.; Grossier, R.; Garcia, E.; Hoff, C.; Furuta, K.; Okustu, T.; Morin, R.; Veesler, S. *J. Cryst. Growth* **2010**, *312* (7), 939.

(18) Hou, D.; Chang, H. C. *Appl. Phys. Lett.* **2008**, *92* (22), 23.

(19) Pareja-Rivera, C.; Cuéllar-Cruz, M.; Esturau-Escofet, N.; Demitri, N.;

Polentarutti, M.; Stojanoff, V.; Moreno, A. *Cryst. Growth Des.* **2016**, *17*, 135.

(20) Koizumi, H.; Uda, S.; Fujiwara, K.; Tachibana, M.; Kojima, K.; Nozawa, J. *J. Appl. Crystallogr.* **2013**, *46* (1), 25.

(21) Koizumi, H.; Suzuki, R.; Tachibana, M.; Tsukamoto, K.; Yoshizaki, I.; Fukuyama, S.; Suzuki, Y.; Uda, S.; Kojima, K. *Cryst. Growth Des.* **2016**, *16*, 4905.

(22) Oxtoby, D. W. *Annu. Rev. Mater. Res.* **2002**, *32*, 39.

(23) Hammadi, Z.; Veesler, S. *Prog. Biophys. Mol. Biol.* **2009**, *101* (1–3), 38.

(24) Nanev, C. N.; Penkova, A. *Colloids Surfaces A Physicochem. Eng. Asp.* **2002**, *209* (2–3), 139.

(25) Ferreira, C. F. D. G.; Camargo, P. C.; Benelli, E. M. *J. Phys. Chem. B* **2015**, *119* (39), 12561.

(26) Guimarães, B. G.; Sanfelici, L.; Neuenschwander, R. T.; Rodrigues, F.; Grizolli, W. C.; Raulik, M. A.; Piton, J. R.; Meyer, B. C.; Nascimento, A. S.; Polikarpov, I. *J. Synchrotron Radiat.* **2008**, *16* (1), 69.

(27) Kim, D. T.; Blanch, H. W.; Radke, C. J. **2002**, *2* (21), 5841.

(28) Westwood, M.; Kirby, A. R.; Parker, R.; Morris, V. J. *Carbohydr. Polym.* **2012**, *89* (4), 1222.

(29) Kubiak-Ossowska, K.; Mulheran, P. A. *Langmuir* **2010**, *26* (20), 15954.

(30) Phillips, D. C. *Proc. Natl. Acad. Sci. U. S. A.* **1967**, *57* (3), 484.

(31) Ferreira, C. F. G.; Benelli, E. M.; Klein, J. J.; Schreiner, W.; Camargo, P. C. *Colloids Surfaces B Biointerfaces* **2009**, *73* (2), 289.

(32) Jackson, M.; Mantsch, H. H. *Crit. Rev. Biochem. Mol. Biol.* **1995**, *30* (2), 95.

(33) Byler, D. M.; Susi, H. *Biopolymers* **1986**, *25* (3), 469.

(34) Goormaghtigh, E.; Cabiaux, V.; Ruysschaert, J.-M. *Eur. Jounal Biochem.* **1990**, *193*, 409.

(35) Pechkova, E.; Innocenzi, P.; Malfatti, L.; Kidchob, T.; Gaspa, L.; Nicolini, C. *Langmuir* **2007**, *23* (3), 1147.

(36) Evans, P. R.; Murshudov, G. N. *Acta Crystallogr. Sect. D Biol. Crystallogr.* **2013**, *69* (7), 1204.

(37) Karplus, P. A.; Diederichs, K. *Science (80-.).* **2012**, *336* (6084), 1030.

(38) Karplus, P. A.; Diederichs, K. *Curr. Opin. Struct. Biol.* **2015**, *34*, 60.

(39) Venkataramani, S.; Truntzer, J.; Coleman, D. R. D. R. *J. Pharm. Bioallied Sci.* **2013**, *5* (2), 148.

For table of contents use only

THE USE OF PROTEIN THIN FILM ORGANIZED BY EXTERNAL ELECTRIC FIELD AS TEMPLATE FOR PROTEIN CRYSTALLIZATION

*Tássia Karina Walter[1], Cecília Fabiana da Gama Ferreira[2], Jorge Iulek[3] and †Elaine Machado Benelli[1]

Table of Contents Graphics and Synopsis

The use of a protein thin film organized by external electric field as template for crystal growth is shown. From our results, the method increases nucleation, improve size and/or morphology of crystals and also contributes to obtain higher crystal quality, as observed by X-ray diffraction analyses.

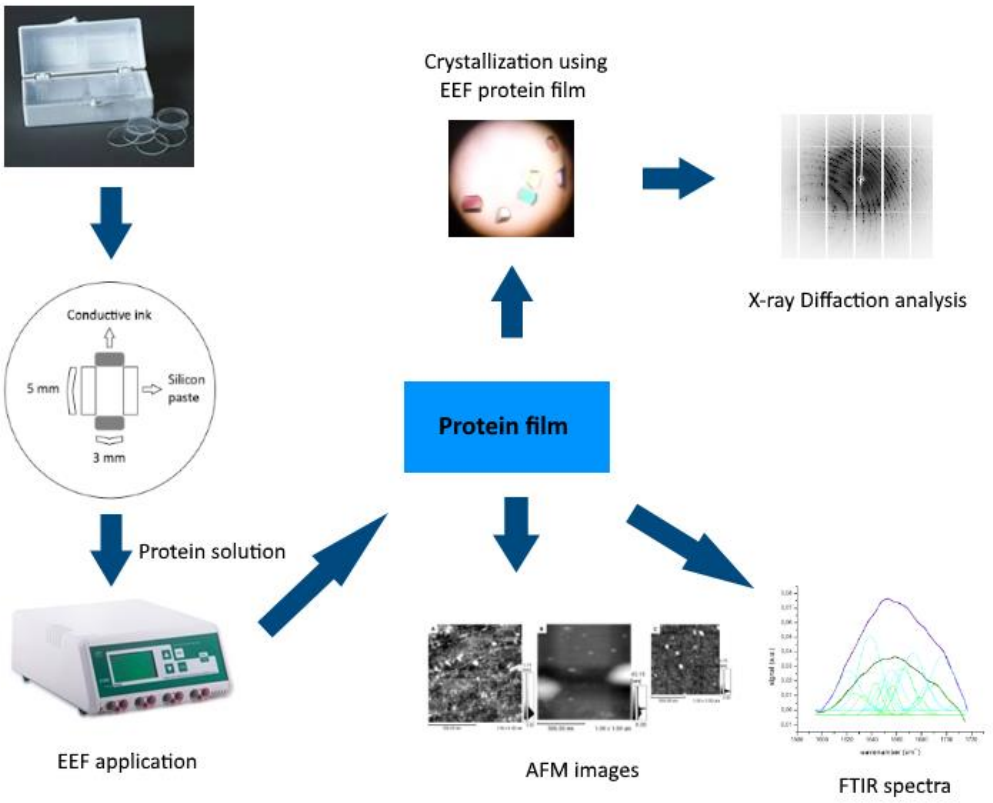

Supplementary material

THE USE OF PROTEIN THIN FILM ORGANIZED BY EXTERNAL ELECTRIC FIELD AS TEMPLATE FOR PROTEIN CRYSTALLIZATION

*Tássia Karina Walter[1], Cecília Fabiana da Gama Ferreira[2], Jorge Iulek[3] and †Elaine Machado Benelli[1]

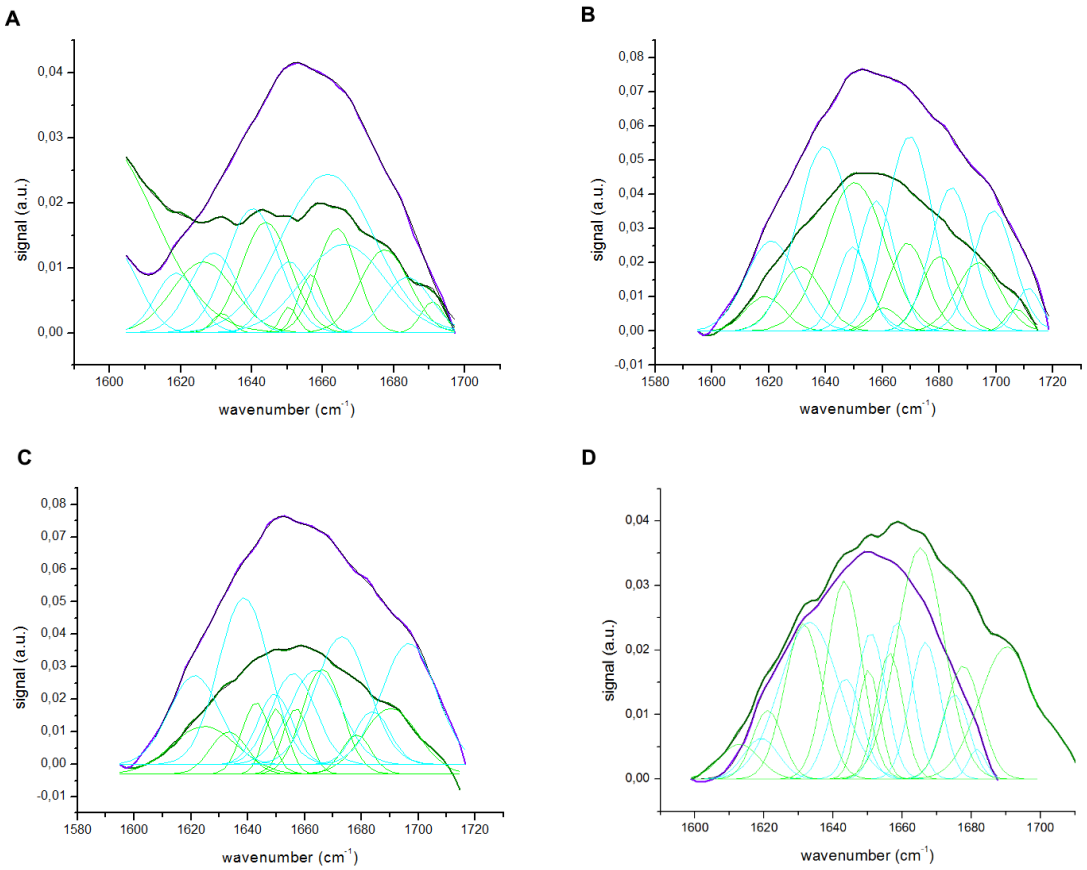

Figure S5. FTIR average spectra of lysozyme thin films formed by drop deposition (violet) and by EEF application (olive) with their respective Gaussian fitting curves (cyan for drop deposition films and green for EEF films). Lysozyme films in sodium acetate buffer, pH 4.5 (a); in phosphate buffer, pH 6.5 (b); in MES buffer, pH 6.2 (c); and in TRIS-HCl buffer, pH 8.0 (d).

APÊNDICE I – METODOLOGIA PARA A ELABORAÇÃO DOS FILMES FINOS DE PROTEÍNA ORGANIZADOS POR CAMPO ELÉTRICO

1. Preparo das canaletas sobre as lâminas de vidro siliconizadas (Hampton Research HR 3-231, 22 mm), através da aplicação de pasta de silicone nas laterais e tinta condutiva a base de grafite nas extremidades, conforme esquema abaixo:

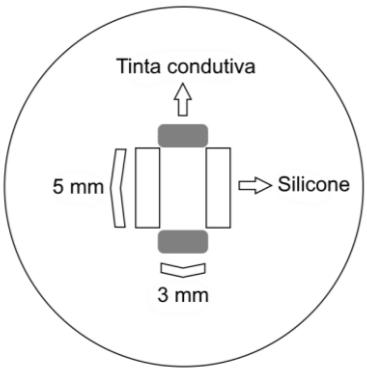

   Obs: as lâminas só deverão ser utilizadas para montagem do filme após completa secagem do silicone e da tinta condutiva.

2. Aplicação da solução contendo a proteína na canaleta, de modo a preencher completamente a área da canaleta (aprox. 20 µl).

3. Encaixe dos fios condutores com garras nas extremidades da lâmina, de modo a manter contato com a tinta condutiva. A lâmina deve ser mantida na posição horizontal.

4. Aplicação do campo elétrico externo de 300 V durante 5 minutos, utilizando uma fonte de eletroforese.

5. Secagem do filme de proteína a temperatura ambiente.

APÊNDICE II – EXPERIMENTOS DE CRISTALIZAÇÃO

Como esta dissertação foi redigida na forma de artigo, sendo necessário resumir consideravelmente os resultados obtidos, nesta seção são apresentados todos os experimentos realizados e as condições empregadas.

Número do experimento	Imagem	Filme Organizado por CEE	Solução de Reservatório	Concentração de Lisozima na Gota	Tempo de surgimento dos cristais	Coleta de dados DRX
1	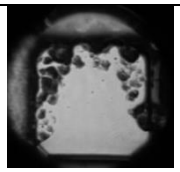	-	50 mM acetato de sódio (pH 4,5), 700 mM NaCl	10 mg/ml	-	-
2	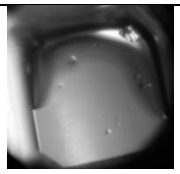	-	50 mM acetato de sódio (pH 4,5), 720 mM NaCl	10 mg/ml	2 semanas	-
3	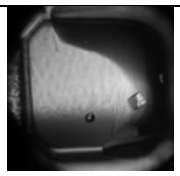	-	50 mM acetato de sódio (pH 4,5), 760 mM NaCl	10 mg/ml	2 semanas	-
4	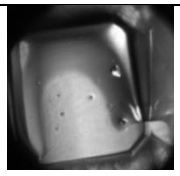	-	50 mM acetato de sódio (pH 4,5), 780 mM NaCl	10 mg/ml	2 semanas	-
5	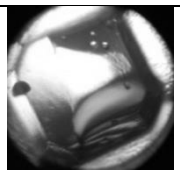	-	50 mM acetato de sódio (pH 4,5), 800 mM NaCl	10 mg/ml	6 semanas	-
6	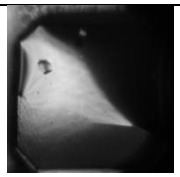	-	50 mM acetato de sódio (pH 4,5), 900 mM NaCl	10 mg/ml	4 semanas	-
7		-	50 mM acetato de sódio (pH 4,5), 1 M NaCl	10 mg/ml	1 semana	-
8	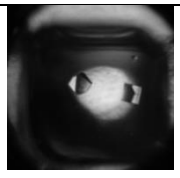	-	50 mM acetato de sódio (pH 4,5), 700 mM NaCl	20 mg/ml	2 semanas	-

Número do experimento	Imagem	Filme Organizado por CEE	Solução de Reservatório	Concentração de Lisozima na Gota	Tempo de surgimento dos cristais	Coleta de dados DRX
9	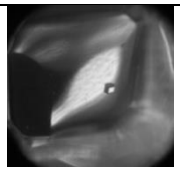	-	50 mM acetato de sódio (pH 4,5), 720 mM NaCl	20 mg/ml	2 semanas	-
10	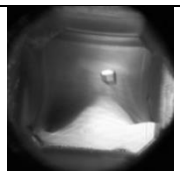	-	50 mM acetato de sódio (pH 4,5), 760 mM NaCl	20 mg/ml	1 semana	-
11	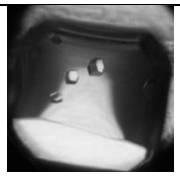	-	50 mM acetato de sódio (pH 4,5), 780 mM NaCl	20 mg/ml	1 semana	1,51 Å
12		-	50 mM acetato de sódio (pH 4,5), 800 mM NaCl	20 mg/ml	1 semana	-
13	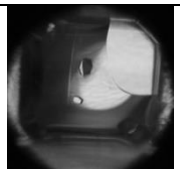	-	50 mM acetato de sódio (pH 4,5), 900 mM NaCl	20 mg/ml	1 semana	-
14	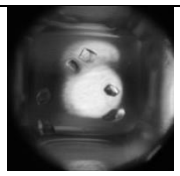	-	50 mM acetato de sódio (pH 4,5), 1 M NaCl	20 mg/ml	1 semana	-
15	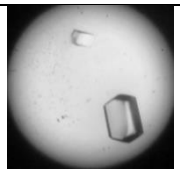	Lisozima (100 nM) em tampão fosfato 50 mM (pH 6,5), NaCl 50 mM	50 mM acetato de sódio (pH 4,5), 500 mM NaCl	10 mg/ml	7 meses	-
16	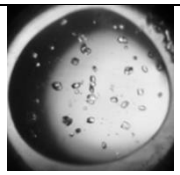	Lisozima (100 nM) em tampão fosfato 50 mM (pH 6,5), NaCl 50 mM	50 mM acetato de sódio (pH 4,5), 600 mM NaCl	10 mg/ml	6 meses	-
17	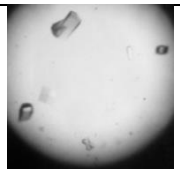	Lisozima (100 nM) em tampão fosfato 50 mM (pH 6,5), NaCl 50 mM	50 mM acetato de sódio (pH 4,5), 700 mM NaCl	10 mg/ml	8 meses	-
18	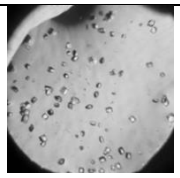	Lisozima (100 nM) em tampão fosfato 50 mM (pH 6,5), NaCl 50 mM	50 mM acetato de sódio (pH 4,5), 720 mM NaCl	10 mg/ml	6 meses	-

Número do experimento	Imagem	Filme Organizado por CEE	Solução de Reservatório	Concentração de Lisozima na Gota	Tempo de surgimento dos cristais	Coleta de dados DRX
19	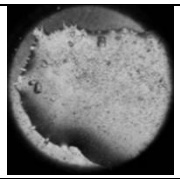	Lisozima (100 nM) em tampão fosfato 50 mM (pH 6,5), NaCl 50 mM	50 mM acetato de sódio (pH 4,5), 760 mM NaCl	10 mg/ml	5 meses	-
20	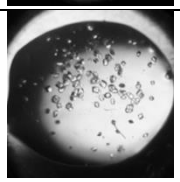	Lisozima (100 nM) em tampão fosfato 50 mM (pH 6,5), NaCl 50 mM	50 mM acetato de sódio (pH 4,5), 780 mM NaCl	10 mg/ml	1 semana	-
21	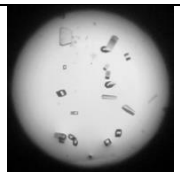	Lisozima (100 nM) em tampão fosfato 50 mM (pH 6,5), NaCl 50 mM	50 mM acetato de sódio (pH 4,5), 800 mM NaCl	10 mg/ml	7 meses	-
22	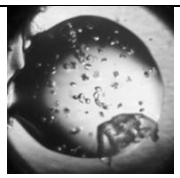	Lisozima (100 nM) em tampão fosfato 50 mM (pH 6,5), NaCl 50 mM	50 mM acetato de sódio (pH 4,5), 900 mM NaCl	10 mg/ml	1 mês	-
23	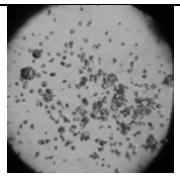	Lisozima (100 nM) em tampão fosfato 50 mM (pH 6,5), NaCl 50 mM	50 mM acetato de sódio (pH 4,5), 1 M NaCl	10 mg/ml	1 semana	-
24	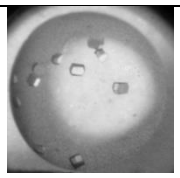	Lisozima (100 nM) em tampão fosfato 50 mM (pH 6,5), NaCl 50 mM	50 mM acetato de sódio (pH 4,5), 780 mM NaCl	20 mg/ml	2 meses	-
25	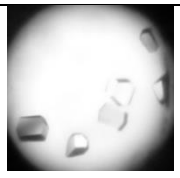	Lisozima (100 nM) em tampão fosfato 50 mM (pH 6,5), NaCl 50 mM	50 mM acetato de sódio (pH 4,5), 900 mM NaCl	20 mg/ml	1 semana	2,52 Å
26	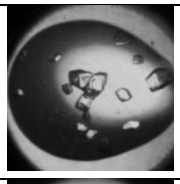	Lisozima (100 nM) em tampão fosfato 50 mM (pH 6,5), NaCl 50 mM	50 mM acetato de sódio (pH 4,5), 1 M NaCl	20 mg/ml	1 semana	-
27	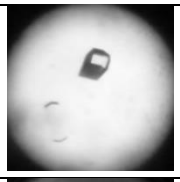	Lisozima (100 nM) em tampão acetato 50 mM (pH 4,5), NaCl 50 mM	50 mM acetato de sódio (pH 4,5), 780 mM NaCl	20 mg/ml	3 semanas	-
28	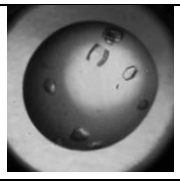	Lisozima (100 nM) em tampão acetato 50 mM (pH 4,5), NaCl 50 mM	50 mM acetato de sódio (pH 4,5), 900 mM NaCl	20 mg/ml	1 semana	1,92 Å

Número do experimento	Imagem	Filme Organizado por CEE	Solução de Reservatório	Concentração de Lisozima na Gota	Tempo de surgimento dos cristais	Coleta de dados DRX
29	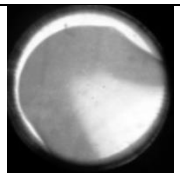	Lisozima (100 nM) em tampão acetato 50 mM (pH 4,5), NaCl 50 mM	50 mM acetato de sódio (pH 4,5), 1 M NaCl	20 mg/ml	4 meses	-
30	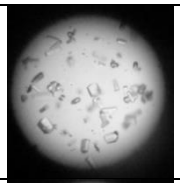	Lisozima (100 nM) em tampão fosfato 50 mM (pH 6,5), NaCl 50 mM	50 mM acetato de sódio (pH 4,5), 780 mM NaCl	10 mg/ml	1 mês	1,68 Å
31	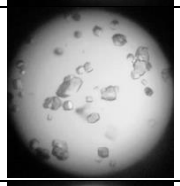	Lisozima (100 nM) em tampão fosfato 50 mM (pH 6,5), NaCl 50 mM	50 mM acetato de sódio (pH 4,5), 900 mM NaCl	10 mg/ml	1 semana	-
32	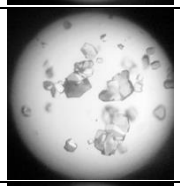	Lisozima (100 nM) em tampão fosfato 50 mM (pH 6,5), NaCl 50 mM	50 mM acetato de sódio (pH 4,5), 1 M NaCl	10 mg/ml	1 semana	-
33	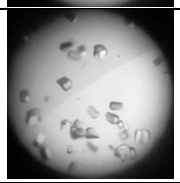	Lisozima (100 nM) em tampão acetato 50 mM (pH 4,5), NaCl 50 mM	50 mM acetato de sódio (pH 4,5), 780 mM NaCl	10 mg/ml	1 mês	-
34	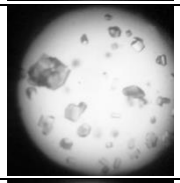	Lisozima (100 nM) em tampão acetato 50 mM (pH 4,5), NaCl 50 mM	50 mM acetato de sódio (pH 4,5), 900 mM NaCl	10 mg/ml	1 semana	-
35	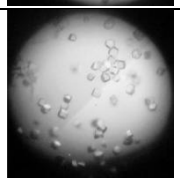	Lisozima (100 nM) em tampão acetato 50 mM (pH 4,5), NaCl 50 mM	50 mM acetato de sódio (pH 4,5), 1 M NaCl	10 mg/ml	1 mês	-
36	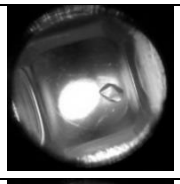	-	50 mM MES (pH 6,2), 700 mM NaCl	10 mg/ml	1 mês	-
37	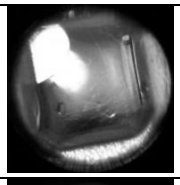	-	50 mM MES (pH 6,2), 720 mM NaCl	10 mg/ml	1 mês	-
38	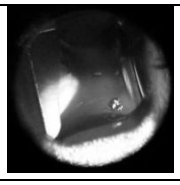	-	50 mM MES (pH 6,2), 760 mM NaCl	10 mg/ml	1 mês	-

Número do experimento	Imagem	Filme Organizado por CEE	Solução de Reservatório	Concentração de Lisozima na Gota	Tempo de surgimento dos cristais	Coleta de dados DRX
39	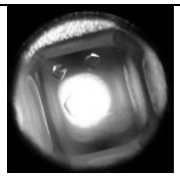	-	50 mM MES (pH 6,2), 780 mM NaCl	10 mg/ml	1 mês	-
40	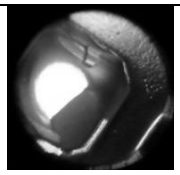	-	50 mM MES (pH 6,2), 800 mM NaCl	10 mg/ml	1 mês	-
41	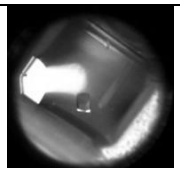	-	50 mM MES (pH 6,2), 900 mM NaCl	10 mg/ml	1 mês	-
42	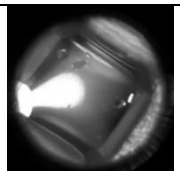	-	50 mM MES (pH 6,2), 1 M NaCl	10 mg/ml	1 mês	-
43		-	50 mM MES (pH 6,2), 700 mM NaCl	20 mg/ml	1 mês	-
44	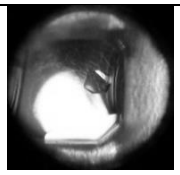	-	50 mM MES (pH 6,2), 720 mM NaCl	20 mg/ml	1 mês	-
45		-	50 mM MES (pH 6,2), 760 mM NaCl	20 mg/ml	1 mês	-
46	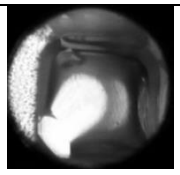	-	50 mM MES (pH 6,2), 780 mM NaCl	20 mg/ml	1 mês	-
47	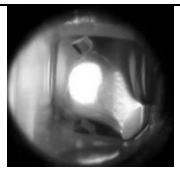	-	50 mM MES (pH 6,2), 800 mM NaCl	20 mg/ml	1 mês	-
48	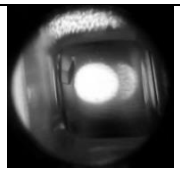	-	50 mM MES (pH 6,2), 900 mM NaCl	20 mg/ml	1 mês	-

Número do experimento	Imagem	Filme Organizado por CEE	Solução de Reservatório	Concentração de Lisozima na Gota	Tempo de surgimento dos cristais	Coleta de dados DRX
49	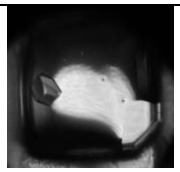	-	50 mM MES (pH 6,2), 1 M NaCl	20 mg/ml	1 semana	3,42 Å
50	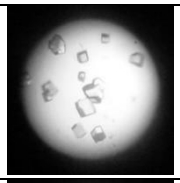	Lisozima (100 nM) em tampão fosfato 50 mM (pH 6,5), NaCl 50 mM	50 mM MES (pH 6,2), 780 mM NaCl	10 mg/ml	1 mês	1,67 Å
51	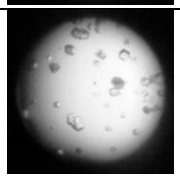	Lisozima (100 nM) em tampão fosfato 50 mM (pH 6,5), NaCl 50 mM	50 mM MES (pH 6,2), 900 mM NaCl	10 mg/ml	1 mês	1,88 Å
52	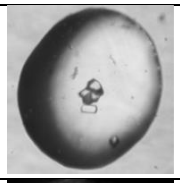	Lisozima (100 nM) em tampão fosfato 50 mM (pH 6,5), NaCl 50 mM	50 mM MES (pH 6,2), 900 mM NaCl	20 mg/ml	1 semana	-
53	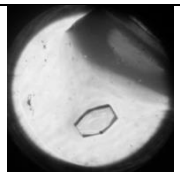	Lisozima (100 nM) em tampão fosfato 50 mM (pH 6,5), NaCl 50 mM	50 mM MES (pH 6,2), 1 M NaCl	20 mg/ml	3 meses	1,60 Å
54	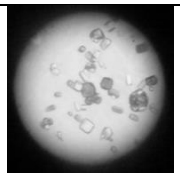	Lisozima (100 nM) em tampão MES 50 mM (pH 6,2), NaCl 50 mM	50 mM MES (pH 6,2), 780 mM NaCl	10 mg/ml	1 mês	1,77 Å
55	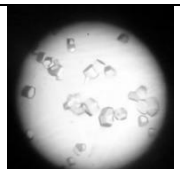	Lisozima (100 nM) em tampão MES 50 mM (pH 6,2), NaCl 50 mM	50 mM MES (pH 6,2), 1 M NaCl	10 mg/ml	1 semana	1,79 Å
56	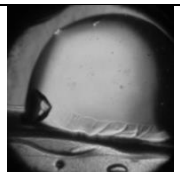	Lisozima (100 nM) em tampão MES 50 mM (pH 6,2), NaCl 50 mM	50 mM MES (pH 6,2), 780 mM NaCl	20 mg/ml	2 meses	-
57	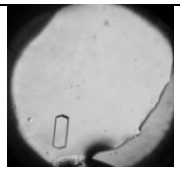	Lisozima (100 nM) em tampão MES 50 mM (pH 6,2), NaCl 50 mM	50 mM MES (pH 6,2), 900 mM NaCl	20 mg/ml	6 meses	-
58	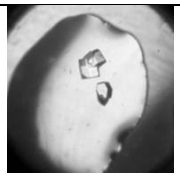	Lisozima (100 nM) em tampão MES 50 mM (pH 6,2), NaCl 50 mM	50 mM MES (pH 6,2), 900 mM NaCl	20 mg/ml	1 semana	-

Número do experimento	Imagem	Filme Organizado por CEE	Solução de Reservatório	Concentração de Lisozima na Gota	Tempo de surgimento dos cristais	Coleta de dados DRX
59		-	50 mM TRIS-HCl (pH 8,0), 700 mM NaCl	10 mg/ml	1 mês	-
60	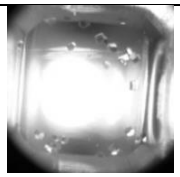	-	50 mM TRIS-HCl (pH 8,0), 720 mM NaCl	10 mg/ml	1 mês	-
61	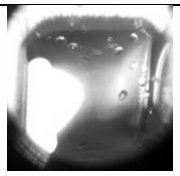	-	50 mM TRIS-HCl (pH 8,0), 760 mM NaCl	10 mg/ml	1 mês	-
62	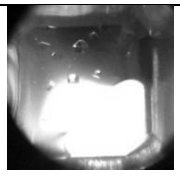	-	50 mM TRIS-HCl (pH 8,0), 780 mM NaCl	10 mg/ml	1 semana	-
63		-	50 mM TRIS-HCl (pH 8,0), 800 mM NaCl	10 mg/ml	1 mês	-
64	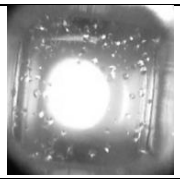	-	50 mM TRIS-HCl (pH 8,0), 900 mM NaCl	10 mg/ml	1 mês	-
65	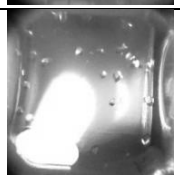	-	50 mM TRIS-HCl (pH 8,0), 1 M NaCl	10 mg/ml	1 mês	-
66	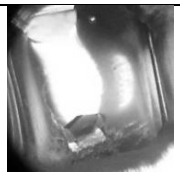	-	50 mM TRIS-HCl (pH 8,0), 720 mM NaCl	20 mg/ml	1 mês	1,52 Å
67	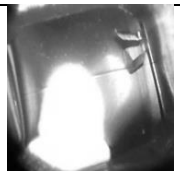	-	50 mM TRIS-HCl (pH 8,0), 760 mM NaCl	20 mg/ml	1 mês	-
68	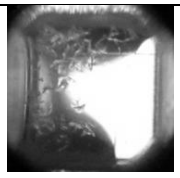	-	50 mM TRIS-HCl (pH 8,0), 780 mM NaCl	20 mg/ml	-	-

Número do experimento	Imagem	Filme Organizado por CEE	Solução de Reservatório	Concentração de Lisozima na Gota	Tempo de surgimento dos cristais	Coleta de dados DRX
69	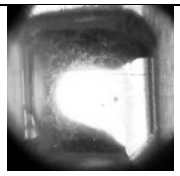	-	50 mM TRIS-HCl (pH 8,0), 800 mM NaCl	20 mg/ml	-	-
70	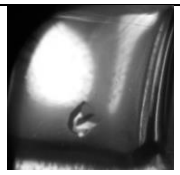	-	50 mM TRIS-HCl (pH 8,0), 900 mM NaCl	20 mg/ml	1 semana	-
71	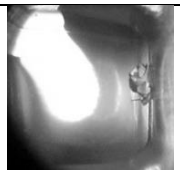	-	50 mM TRIS-HCl (pH 8,0), 1 M NaCl	20 mg/ml	1 mês	-
72	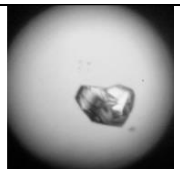	Lisozima (100 nM) em tampão fosfato 50 mM (pH 6,5), NaCl 50 mM	50 mM TRIS-HCl (pH 8,0), 780 mM NaCl	20 mg/ml	2 semanas	-
73	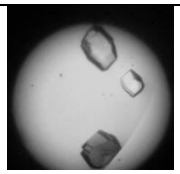	Lisozima (100 nM) em tampão fosfato 50 mM (pH 6,5), NaCl 50 mM	50 mM TRIS-HCl (pH 8,0), 780 mM NaCl	20 mg/ml	1 mês	-
74	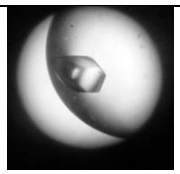	Lisozima (100 nM) em tampão fosfato 50 mM (pH 6,5), NaCl 50 mM	50 mM TRIS-HCl (pH 8,0), 900 mM NaCl	20 mg/ml	1 mês	1,67 Å
75	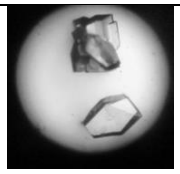	Lisozima (100 nM) em tampão fosfato 50 mM (pH 6,5), NaCl 50 mM	50 mM TRIS-HCl (pH 8,0), 1 M NaCl	20 mg/ml	1 semana	-
76	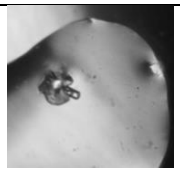	Lisozima (100 nM) em tampão TRIS-HCl 50 mM (pH 8,0), NaCl 50 mM	50 mM TRIS-HCl (pH 8,0), 780 mM NaCl	20 mg/ml	3 meses	1,67 Å
77	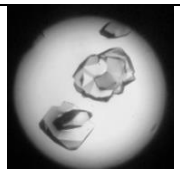	Lisozima (100 nM) em tampão TRIS-HCl 50 mM (pH 8,0), NaCl 50 mM	50 mM TRIS-HCl (pH 8,0), 900 mM NaCl	20 mg/ml	1 semana	-
78	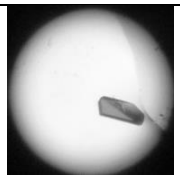	Lisozima (100 nM) em tampão TRIS-HCl 50 mM (pH 8,0), NaCl 50 mM	50 mM TRIS-HCl (pH 8,0), 900 mM NaCl	20 mg/ml	3 meses	-

Número do experimento	Imagem	Filme Organizado por CEE	Solução de Reservatório	Concentração de Lisozima na Gota	Tempo de surgimento dos cristais	Coleta de dados DRX
79	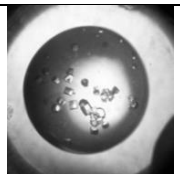	Lisozima (100 nM) em tampão fosfato 50 mM (pH 6,5), NaCl 50 mM	50 mM TRIS-HCl (pH 8,0), 780 mM NaCl	10 mg/ml	1 mês	-
80	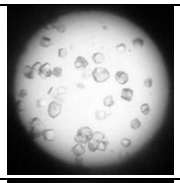	Lisozima (100 nM) em tampão fosfato 50 mM (pH 6,5), NaCl 50 mM	50 mM TRIS-HCl (pH 8,0), 900 mM NaCl	10 mg/ml	1 mês	2,06 Å
81	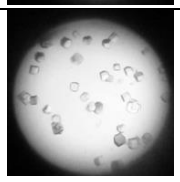	Lisozima (100 nM) em tampão fosfato 50 mM (pH 6,5), NaCl 50 mM	50 mM TRIS-HCl (pH 8,0), 1 M NaCl	10 mg/ml	1 mês	-
82		Lisozima (100 nM) em tampão TRIS-HCl 50 mM (pH 8,0), NaCl 50 mM	50 mM TRIS-HCl (pH 8,0), 900 mM NaCl	10 mg/ml	3 meses	1,88 Å
83	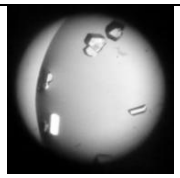	Lisozima (100 nM) em tampão TRIS-HCl 50 mM (pH 8,0), NaCl 50 mM	50 mM TRIS-HCl (pH 8,0), 1 M NaCl	10 mg/ml	1 mês	-
84	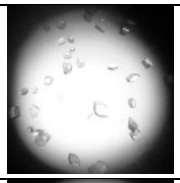	-	100 mM imidazol (pH 6,5), 1 M acetato de sódio	20 mg/ml	1 semana	-
85	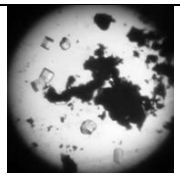	Lisozima (100 nM) em tampão fosfato 50 mM (pH 6,5), NaCl 50 mM	100 mM imidazol (pH 6,5), 1 M acetato de sódio	5 mg/ml	1 semana	-
86	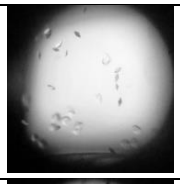	-	0,1M fosfato de sódio, 0,1M fosfato de potássio, 0,1M MES (pH 6,5), 2M NaCl	5 mg/ml	1 semana	-
87	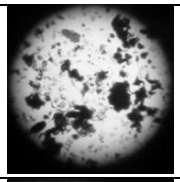	Lisozima (100 nM) em tampão fosfato 50 mM (pH 6,5), NaCl 50 mM	0,1M fosfato de sódio, 0,1M fosfato de potássio, 0,1M MES (pH 6,5), 2M NaCl	5 mg/ml	1 semana	-
88	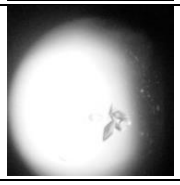	-	0,2M sulfato de amônio, 0,1M MES (pH 6,5), PEG 5000 30%	5 mg/ml	1 semana	-

Número do experimento	Imagem	Filme Organizado por CEE	Solução de Reservatório	Concentração de Lisozima na Gota	Tempo de surgimento dos cristais	Coleta de dados DRX
89	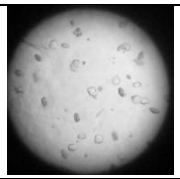	Lisozima (100 nM) em tampão fosfato 50 mM (pH 6,5), NaCl 50 mM	0,2M sulfato de amônio, 0,1M MES (pH 6,5), PEG 5000 30%	5 mg/ml	1 semana	-
90	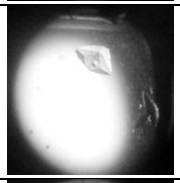	-	0,2M sulfato de amônio, 0,1M MES (pH 6,5), PEG 5000 30%	10 mg/ml	1 semana	-
91	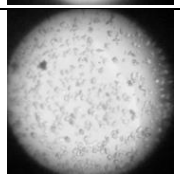	Lisozima (100 nM) em tampão fosfato 50 mM (pH 6,5), NaCl 50 mM	0,2M sulfato de amônio, 0,1M MES (pH 6,5), PEG 5000 30%	20 mg/ml	1 semana	-
92	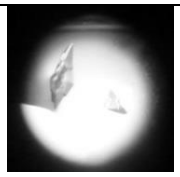	-	0,2M acetato de amônio, 0,1M acetato de sódio (pH 5,6), PEG 4000 30%	20 mg/ml	1 semana	-
93	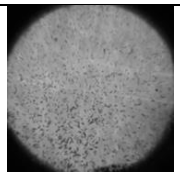	Lisozima (100 nM) em tampão acetato 50 mM (pH 4,5), NaCl 50 mM	0,2M acetato de amônio, 0,1M acetato de sódio (pH 5,6), PEG 4000 30%	20 mg/ml	1 mês	-
94	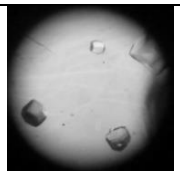	Lisozima (100 nM) em tampão fosfato 50 mM (pH 6,5), NaCl 50 mM	0,1M NaCl, 0,1M HEPES (pH 7,5), 1,6M sulfato de amônio	20 mg/ml	1 semana	-
95	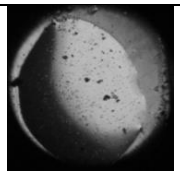	Lisozima (100 nM) em tampão fosfato 50 mM (pH 6,5), NaCl 50 mM	0,2M acetato de magnésio, 0,1M cacodilato de sódio (pH 6,5), PEG 8000 20%	5 mg/ml	2 meses	-
96	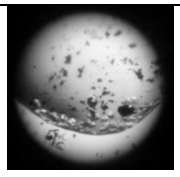	Lisozima (100 nM) em tampão fosfato 50 mM (pH 6,5), NaCl 50 mM	0,2M acetato de magnésio, 0,1M cacodilato de sódio (pH 6,5), PEG 8000 20%	10 mg/ml	1 mês	-

APÊNDICE III – ESTATÍSTICA DO PROCESSAMENTO DE DADOS DE DIFRAÇÃO DE RAIOS-X NAS CAMADAS DE MAIOR RESOLUÇÃO

Nesta seção estão apresentados os principais parâmetros estatísticos obtidos no processamento de dados de difração de raios-X dos cristais analisados, considerando somente as camadas de maior resolução.

Os parâmetros estatísticos podem ser definidos como:

- R-FACTOR
  - observado = $\frac{SUM\left[ABS\left(I(h,i)-I(h)\right)\right]}{SUM\left(I(h,i)\right)}$
  - esperado = R-FACTOR esperado derivado de Sigma(I)
  - COMPARED = número de reflexões usado para calcular R-FACTOR

- I/SIGMA = média de intensidade/Sigma(I) de reflexões únicas (após unir as observações relacionadas à simetria)
- Sigma(I) = desvio padrão da intensidade das reflexões (I) estimado da estatística das amostras
- R-meas = redundância independente de R-factor (intensidade).
  (Diederichs & Karplus (1997), Nature Struct. Biol. 4, 269-275).
- CC(1/2) = percentagem de correlação entre intensidades de meios conjuntos de dados tomados aleatoriamente. Correlação significante superior a 0.1% é marcada com asterisco.
  (Karplus & Diederichs (2012), Science 336, 1030-33).

Tabela 3- Cristal de lisozima em tampão acetato (pH 4.5) sem filme (controle, experimento nº 11)

RESOLUTION	NUMBER OF REFLECTIONS			COMPLETENESS	R-FACTOR					
LIMIT	Observed	Unique	Possible	(%)	Observed	Expected	COMPARED	I/SIGMA	R-meas	CC(1/2)
4.10	6447	1021	1025	99.6%	3.1%	3.8%	6413	46.22	3.4%	99.9*
3.25	6065	960	969	99.1%	3.9%	4.5%	6044	38.19	4.2%	99.7*
2.84	6016	935	951	98.3%	4.7%	5.4%	5998	30.54	5.1%	99.8*
2.58	6107	936	940	99.6%	5.9%	6.4%	6089	25.72	6.3%	99.7*
2.40	5388	878	891	98.5%	7.1%	7.2%	5375	21.36	7.7%	99.7*
2.26	5937	906	916	98.9%	7.6%	7.7%	5927	20.19	8.2%	99.7*
2.14	6011	954	969	98.5%	8.6%	8.6%	5989	17.83	9.3%	99.3*
2.05	5586	864	876	98.6%	9.1%	9.1%	5576	16.53	9.8%	99.6*
1.97	6284	932	939	99.3%	11.0%	10.9%	6267	14.49	11.8%	99.4*
1.90	6243	929	934	99.5%	13.1%	12.8%	6233	12.54	14.0%	99.2*
1.84	5358	907	911	99.6%	16.7%	16.7%	5352	9.54	18.3%	98.7*
1.79	4793	873	879	99.3%	18.7%	19.4%	4783	7.98	20.6%	98.2*
1.74	4732	949	961	98.8%	25.2%	25.4%	4705	6.14	28.2%	93.7*
1.70	3696	838	854	98.1%	28.6%	28.6%	3669	5.34	32.4%	94.0*
1.66	4185	935	938	99.7%	32.3%	34.8%	4168	4.58	36.6%	92.9*
1.63	3185	758	762	99.5%	37.9%	38.4%	3167	4.21	43.4%	86.8*
1.59	3848	1105	1111	99.5%	40.3%	43.5%	3785	3.21	47.5%	87.8*
1.56	2580	896	913	98.1%	43.0%	49.0%	2492	2.33	52.4%	79.5*
1.54	1543	603	644	93.6%	54.9%	59.6%	1445	1.61	68.0%	61.3*
1.51	1604	874	1026	85.2%	51.6%	61.9%	1232	1.04	67.6%	59.1*
total	95608	18053	18409	98.1%	5.4%	6.0%	94709	15.00	5.9%	99.9*

Tabela 2 - Cristal de lisozima em tampão acetato (pH 4.5) utilizando filme de lisozima em tampão fosfato (experimento nº 25)

RESOLUTION	NUMBER OF REFLECTIONS			COMPLETENESS	R-FACTOR					
LIMIT	Observed	Unique	Possible	(%)	Observed	Expected	COMPARED	I/SIGMA	R-meas	CC(1/2)
6.84	1426	245	248	98.8%	13.6%	15.1%	1420	9.22	15.0%	98.2*
5.43	1444	220	220	100.0%	17.5%	19.0%	1441	7.78	19.0%	98.5*
4.74	1256	212	215	98.6%	18.5%	20.6%	1256	6.77	20.4%	97.4*
4.31	1339	210	214	98.1%	20.9%	22.2%	1338	6.62	22.9%	97.1*
4.00	1428	208	211	98.6%	22.1%	23.7%	1428	6.46	24.1%	94.6*
3.76	1395	206	209	98.6%	23.9%	25.7%	1394	5.64	26.0%	96.5*
3.58	1294	194	199	97.5%	26.7%	26.7%	1294	5.47	29.1%	94.7*
3.42	1228	209	215	97.2%	26.2%	26.8%	1218	4.97	28.8%	95.0*
3.29	1241	196	202	97.0%	28.5%	27.8%	1240	4.53	31.2%	94.8*
3.18	1269	197	199	99.0%	30.2%	29.8%	1267	4.56	33.2%	95.5*
3.08	1251	189	192	98.4%	35.6%	36.5%	1250	3.95	38.8%	95.2*
2.99	1407	214	216	99.1%	41.5%	40.2%	1406	3.50	45.4%	90.3*
2.91	1353	202	202	100.0%	46.8%	46.7%	1352	3.15	51.2%	94.4*
2.84	1365	199	203	98.0%	46.6%	47.1%	1365	3.41	50.7%	95.3*
2.77	1445	213	217	98.2%	47.7%	51.0%	1444	3.06	51.8%	93.0*
2.71	1365	196	200	98.0%	57.0%	57.0%	1365	2.97	62.0%	88.1*
2.66	1313	188	190	98.9%	68.9%	68.6%	1312	2.66	74.7%	86.6*

2.61	1185	190	190	100.0%	71.2%	72.9%	1182	2.26	77.9%	84.7*
2.56	1291	222	227	97.8%	63.3%	61.5%	1284	2.55	69.5%	86.5*
2.52	809	160	181	88.4%	101.8%	114.9%	799	1.40	113.0%	78.5*
total	26104	4070	4150	98.1%	26.3%	27.3%	26055	4.66	28.7%	96.9*

Tabela 3 - Cristal de lisozima em tampão acetato (pH 4.5) utilizando filme de lisozima em tampão acetato (experimento nº 28)

RESOLUTION	NUMBER OF REFLECTIONS			COMPLETENESS	R-FACTOR					
LIMIT	Observed	Unique	Possible	(%)	Observed	Expected	COMPARED	I/SIGMA	R-meas	CC(1/2)
4.40	5266	843	847	99.5%	6.6%	7.0%	5262	21.16	7.2%	99.5*
3.49	5228	775	788	98.4%	7.7%	8.1%	5226	18.60	8.3%	99.5*
3.05	4839	756	762	99.2%	10.5%	10.7%	4831	13.76	11.4%	99.3*
2.77	5208	758	765	99.1%	16.9%	17.0%	5206	9.67	18.3%	98.7*
2.57	5211	769	771	99.7%	22.4%	22.6%	5205	7.77	24.2%	97.6*
2.42	4792	737	740	99.6%	29.3%	29.5%	4789	5.97	31.9%	96.4*
2.30	5069	730	731	99.9%	40.2%	40.2%	5066	4.80	43.4%	92.6*
2.20	5147	745	746	99.9%	47.9%	47.4%	5145	4.08	51.8%	93.6*
2.11	4982	779	788	98.9%	70.3%	70.0%	4978	2.62	76.6%	81.8*
2.04	4832	714	714	100.0%	83.4%	81.5%	4828	2.32	90.3%	73.9*
1.98	4825	698	698	100.0%	98.2%	98.1%	4824	1.86	106.2%	77.6*
1.92	5182	770	773	99.6%	172.7%	172.7%	5174	1.09	187.1%	57.2*
total	60581	9074	9123	99.5%	16.2%	16.4%	60534	8.02	17.5%	99.4*

Tabela 4 - Cristal de lisozima em tampão acetato (pH 4.5) utilizando filme de lisozima em tampão fosfato (experimento nº 30)

RESOLUTION	NUMBER OF REFLECTIONS			COMPLETENESS	R-FACTOR					
LIMIT	Observed	Unique	Possible	(%)	Observed	Expected	COMPARED	I/SIGMA	R-meas	CC(1/2)
4.56	4653	756	764	99.0%	3.5%	3.9%	4624	38.20	3.8%	99.9*
3.62	4745	702	706	99.4%	3.8%	4.2%	4737	37.70	4.1%	99.9*
3.16	4195	685	693	98.8%	4.7%	5.0%	4174	28.24	5.1%	99.7*
2.87	4612	685	693	98.8%	7.3%	7.3%	4598	20.85	7.8%	99.8*
2.67	4638	659	662	99.5%	10.4%	10.4%	4627	16.30	11.2%	99.5*
2.51	4332	683	686	99.6%	13.0%	12.9%	4319	13.01	14.2%	98.8*
2.38	4575	691	693	99.7%	15.4%	15.2%	4565	11.42	16.6%	98.9*
2.28	4368	644	645	99.8%	17.4%	17.1%	4359	10.45	18.8%	98.4*
2.19	4736	690	693	99.6%	19.1%	18.9%	4732	9.58	20.6%	98.1*
2.12	3860	611	613	99.7%	21.3%	21.4%	3853	8.05	23.1%	98.1*
2.05	4600	684	689	99.3%	24.5%	24.2%	4598	7.51	26.5%	97.4*
1.99	4828	697	699	99.7%	30.3%	30.4%	4824	6.27	32.6%	95.9*
1.94	4378	629	629	100.0%	38.5%	38.3%	4372	5.15	41.4%	93.5*
1.89	4600	703	703	100.0%	42.1%	41.8%	4593	4.71	45.6%	93.1*
1.85	3577	604	606	99.7%	55.5%	55.7%	3572	3.35	60.9%	83.9*
1.81	3744	671	673	99.7%	58.6%	59.7%	3735	3.03	64.7%	83.8*
1.77	3782	710	718	98.9%	73.9%	74.7%	3774	2.40	82.0%	73.8*
1.74	2821	593	596	99.5%	89.8%	91.3%	2814	1.79	101.0%	63.9*
1.71	2873	641	643	99.7%	97.0%	96.6%	2860	1.65	109.8%	58.8*

1.68	2966	664	669	99.3%	117.0%	118.5%	2949	1.38	132.6%	51.5*
total	82883	13402	13473	99.5%	9.6%	9.8%	82679	11.91	10.4%	99.8*

Tabela 5 - Cristal de lisozima em tampão MES (pH 6.2) sem filme (controle, experimento nº 49)

RESOLUTION	NUMBER OF REFLECTIONS			COMPLETENESS	R-FACTOR					
LIMIT	Observed	Unique	Possible	(%)	Observed	Expected	COMPARED	I/SIGMA	R-meas	CC(1/2)
7.11	1076	207	216	95.8%	28.9%	31.4%	1068	3.38	32.5%	94.6*
5.65	1191	183	197	92.9%	44.5%	46.9%	1191	2.69	48.5%	92.1*
4.93	945	174	192	90.6%	57.3%	53.2%	944	2.18	63.8%	87.0*
4.48	1088	182	185	98.4%	47.6%	46.4%	1086	2.41	51.9%	92.7*
4.16	1219	186	186	100.0%	36.5%	35.5%	1218	3.64	39.4%	94.8*
3.92	1128	171	175	97.7%	38.0%	38.4%	1126	3.45	41.0%	93.4*
3.72	1163	172	178	96.6%	37.0%	36.2%	1161	3.52	39.8%	96.2*
3.56	1149	177	180	98.3%	46.4%	43.2%	1148	2.69	50.2%	93.2*
3.42	1056	180	183	98.4%	44.5%	40.9%	1051	2.79	48.6%	92.8*
total	10015	1632	1692	96.5%	37.5%	37.5%	9993	2.98	41.0%	94.6*

Tabela 6 - Cristal de lisozima em tampão MES (pH 6.2) utilizando filme de lisozima em tampão fosfato (experimento nº 50)

RESOLUTION	NUMBER OF REFLECTIONS			COMPLETENESS	R-FACTOR					
LIMIT	Observed	Unique	Possible	(%)	Observed	Expected	COMPARED	I/SIGMA	R-meas	CC(1/2)
4.53	4877	776	781	99.4%	3.4%	3.5%	4872	43.72	3.7%	99.9*
3.60	4974	707	710	99.6%	3.2%	3.5%	4974	46.88	3.4%	99.9*
3.14	4521	714	716	99.7%	3.8%	4.0%	4520	37.61	4.1%	99.9*
2.86	4723	679	682	99.6%	5.5%	5.7%	4720	28.41	5.9%	99.9*
2.65	4992	701	701	100.0%	7.5%	7.6%	4992	22.91	8.1%	99.7*
2.49	4551	711	711	100.0%	9.0%	9.1%	4548	18.56	9.8%	99.4*
2.37	4469	651	651	100.0%	10.7%	10.7%	4468	16.72	11.6%	99.4*
2.27	4683	663	663	100.0%	12.0%	12.0%	4681	15.65	12.9%	99.2*
2.18	4674	693	693	100.0%	15.2%	15.2%	4670	12.23	16.4%	98.6*
2.10	4795	734	734	100.0%	18.3%	18.6%	4794	10.01	19.9%	98.4*
2.04	4214	610	610	100.0%	21.6%	21.9%	4214	8.96	23.4%	97.4*
1.98	4824	698	698	100.0%	26.8%	26.4%	4824	7.48	29.0%	96.1*
1.93	4471	642	643	99.8%	39.1%	38.7%	4471	5.23	42.2%	93.1*
1.88	4402	705	706	99.9%	35.8%	36.6%	4398	5.08	39.1%	93.4*
1.84	3607	621	622	99.8%	53.4%	53.2%	3599	3.42	58.5%	85.0*
1.80	3871	695	697	99.7%	56.0%	55.4%	3857	3.20	61.8%	83.6*
1.76	3852	748	749	99.9%	68.9%	70.6%	3835	2.37	76.7%	71.6*
1.73	2666	595	597	99.7%	87.4%	87.4%	2656	1.80	99.2%	55.6*
1.70	3024	649	651	99.7%	94.3%	95.1%	3009	1.70	106.2%	58.4*
1.67	3006	687	696	98.7%	107.3%	104.5%	2978	1.43	121.9%	51.5*
total	85196	13679	13711	99.8%	7.5%	7.7%	85080	15.09	8.2%	99.9*

Tabela 7 - Cristal de lisozima em tampão MES (pH 6.2) utilizando filme de lisozima em tampão fosfato (experimento nº 51)

RESOLUTION	NUMBER OF REFLECTIONS			COMPLETENESS	R-FACTOR					
LIMIT	Observed	Unique	Possible	(%)	Observed	Expected	COMPARED	I/SIGMA	R-meas	CC(1/2)
5.10	3444	551	556	99.1%	7.3%	7.7%	3441	19.30	7.9%	99.5*
4.05	3402	512	512	100.0%	8.2%	8.5%	3400	18.43	8.9%	99.5*
3.54	3466	500	500	100.0%	9.1%	9.4%	3466	17.07	9.8%	99.3*
3.21	3004	502	505	99.4%	10.5%	11.1%	3002	13.34	11.6%	98.8*
2.98	3253	484	486	99.6%	13.9%	14.2%	3251	11.36	15.1%	99.0*
2.81	3276	472	472	100.0%	18.6%	19.3%	3274	8.87	20.2%	98.1*
2.67	3156	486	487	99.8%	24.3%	22.1%	3156	7.61	26.5%	96.6*
2.55	3307	493	493	100.0%	27.1%	28.3%	3306	6.49	29.4%	95.5*
2.45	3136	489	489	100.0%	33.0%	33.3%	3134	5.50	35.9%	94.9*
2.37	3035	452	452	100.0%	37.4%	37.0%	3034	5.19	40.5%	92.5*
2.29	3586	513	513	100.0%	41.2%	42.1%	3586	4.68	44.5%	93.6*
2.23	3141	449	449	100.0%	48.5%	47.4%	3139	4.22	52.4%	91.5*
2.17	3268	482	482	100.0%	56.2%	56.2%	3267	3.59	61.0%	89.9*
2.12	2826	451	452	99.8%	64.7%	65.6%	2824	2.98	70.7%	87.6*
2.07	3324	496	499	99.4%	70.2%	69.8%	3323	2.89	76.1%	82.4*
2.03	2856	421	421	100.0%	91.7%	94.6%	2856	2.17	99.3%	74.7*
1.98	3980	575	582	98.8%	140.9%	151.0%	3980	1.37	152.5%	73.1*
1.95	2211	362	373	97.1%	94.6%	75.6%	2211	2.59	103.5%	73.2*
1.91	3687	530	541	98.0%	251.2%	250.8%	3685	0.90	271.8%	61.6*
1.88	2822	435	435	100.0%	170.5%	187.7%	2820	1.09	185.4%	50.9*
total	64180	9655	9699	99.5%	19.0%	19.3%	64155	7.18	20.7%	99.3*

Tabela 8 - Cristal de lisozima em tampão MES (pH 6.2) utilizando filme de lisozima em tampão fosfato (experimento nº 53)

RESOLUTION	NUMBER OF REFLECTIONS			COMPLETENESS	R-FACTOR					
LIMIT	Observed	Unique	Possible	(%)	Observed	Expected	COMPARED	I/SIGMA	R-meas	CC(1/2)
3.95	6966	1111	1145	97.0%	8.9%	11.3%	6961	14.94	9.8%	98.8*
3.13	6264	1046	1075	97.3%	11.2%	14.1%	6258	10.89	12.2%	99.1*
2.74	6623	1030	1050	98.1%	16.5%	18.9%	6619	7.61	18.0%	98.2*
2.49	6435	1019	1031	98.8%	20.9%	23.0%	6431	6.19	22.8%	97.8*
2.31	6838	1029	1038	99.1%	25.2%	26.2%	6836	5.85	27.4%	97.0*
2.17	6981	1050	1057	99.3%	27.9%	28.9%	6976	5.64	30.3%	95.6*
2.06	6629	1034	1039	99.5%	30.3%	30.9%	6627	5.22	33.0%	94.8*
1.97	7057	1030	1041	98.9%	37.3%	37.8%	7057	4.71	40.3%	94.5*
1.90	6334	927	934	99.3%	40.4%	43.5%	6334	4.21	43.7%	94.4*
1.83	6368	1082	1090	99.3%	50.1%	54.1%	6365	3.21	55.1%	89.4*
1.77	5685	1049	1065	98.5%	63.7%	67.5%	5679	2.58	70.7%	85.6*
1.72	4770	1009	1022	98.7%	70.8%	74.5%	4744	2.19	80.0%	76.6*
1.68	3990	871	886	98.3%	96.0%	99.8%	3970	1.69	109.2%	73.5*
1.64	4220	954	984	97.0%	93.1%	101.8%	4188	1.58	106.3%	61.3*
1.60	4062	1070	1075	99.5%	92.9%	97.4%	4005	1.58	108.7%	50.8*
total	89222	15311	15532	98.6%	15.2%	17.6%	89050	5.31	16.6%	99.2*

Tabela 9 - Cristal de lisozima em tampão MES (pH 6.2) utilizando filme de lisozima em tampão MES (experimento nº 54)

RESOLUTION	NUMBER OF REFLECTIONS			COMPLETENESS	R-FACTOR					
LIMIT	Observed	Unique	Possible	(%)	Observed	Expected	COMPARED	I/SIGMA	R-meas	CC(1/2)
4.80	4148	622	664	93.7%	5.0%	5.5%	4124	28.55	5.4%	99.6*
3.81	3877	585	610	95.9%	5.5%	6.3%	3864	24.37	5.9%	99.8*
3.33	3445	571	582	98.1%	6.3%	7.0%	3434	21.03	6.8%	99.7*
3.03	3654	569	589	96.6%	7.7%	8.3%	3642	18.50	8.4%	99.3*
2.81	4030	581	586	99.1%	10.4%	10.7%	4016	14.88	11.2%	99.3*
2.64	4118	593	599	99.0%	11.9%	12.5%	4102	13.50	12.9%	99.0*
2.51	3553	567	574	98.8%	14.0%	14.1%	3538	11.82	15.3%	98.4*
2.40	3829	563	572	98.4%	15.6%	16.0%	3823	10.72	16.9%	98.7*
2.31	3958	558	563	99.1%	17.6%	17.6%	3956	10.65	18.9%	98.3*
2.23	4040	572	575	99.5%	20.0%	20.4%	4027	9.44	21.6%	97.7*
2.16	3574	557	557	100.0%	23.0%	23.1%	3572	8.07	25.0%	96.8*
2.10	3736	570	571	99.8%	25.1%	25.8%	3728	7.34	27.2%	97.5*
2.04	4276	610	610	100.0%	30.3%	29.9%	4276	6.68	32.7%	96.4*
1.99	4027	584	584	100.0%	36.2%	36.4%	4024	5.57	39.2%	94.7*
1.95	3445	487	487	100.0%	45.3%	45.5%	3444	4.65	48.8%	92.2*
1.91	3558	541	541	100.0%	52.5%	52.1%	3558	3.89	57.1%	91.4*
1.87	3512	597	597	100.0%	53.9%	54.3%	3509	3.41	59.2%	86.1*
1.83	3583	638	639	99.8%	80.4%	81.7%	3579	2.22	88.9%	72.7*
1.80	2799	518	518	100.0%	74.4%	74.9%	2798	2.31	82.5%	75.5*
1.77	2557	540	547	98.7%	98.3%	97.5%	2542	1.67	110.7%	53.5*
total	73719	11423	11565	98.8%	10.7%	11.3%	73556	10.61	11.7%	99.7*

Tabela 10 - Cristal de lisozima em tampão MES (pH 6.2) utilizando filme de lisozima em tampão MES (experimento nº 55)

RESOLUTION	NUMBER OF REFLECTIONS			COMPLETENESS	R-FACTOR					
LIMIT	Observed	Unique	Possible	(%)	Observed	Expected	COMPARED	I/SIGMA	R-meas	CC(1/2)
4.86	3814	577	636	90.7%	7.4%	8.0%	3765	19.78	8.0%	99.3*
3.86	3783	562	595	94.5%	7.7%	8.9%	3733	18.21	8.3%	99.3*
3.37	3479	544	571	95.3%	8.5%	9.7%	3428	15.77	9.2%	99.5*
3.06	3500	551	569	96.8%	10.2%	11.0%	3468	13.27	11.0%	99.2*
2.84	3816	560	574	97.6%	13.8%	14.5%	3776	10.29	14.7%	99.1*
2.67	4014	565	573	98.6%	15.5%	16.3%	3977	9.38	16.6%	98.6*
2.54	3445	537	543	98.9%	20.1%	20.0%	3412	7.74	21.6%	97.3*
2.43	3514	540	545	99.1%	22.6%	23.3%	3479	6.53	24.3%	97.9*
2.34	3720	539	542	99.4%	25.1%	25.2%	3686	6.42	26.9%	97.1*
2.26	3709	540	544	99.3%	26.9%	27.1%	3677	5.92	28.9%	97.8*
2.18	4219	614	616	99.7%	32.4%	32.6%	4184	5.09	34.7%	95.7*
2.12	3309	531	540	98.3%	38.8%	39.4%	3282	4.11	41.9%	95.2*
2.07	3321	494	499	99.0%	39.8%	39.1%	3297	4.17	42.8%	93.5*
2.02	3581	524	530	98.9%	52.4%	51.8%	3554	3.34	56.3%	90.7*
1.97	4209	591	599	98.7%	54.1%	54.4%	4182	3.20	57.9%	90.7*
1.93	3546	514	517	99.4%	75.4%	76.7%	3522	2.29	81.0%	80.5*

1.89	3766	569	575	99.0%	66.6%	64.5%	3742	2.55	71.8%	86.4*
1.85	3566	599	606	98.8%	116.9%	120.4%	3536	1.42	127.3%	65.4*
1.82	2643	473	487	97.1%	140.5%	138.7%	2617	1.28	153.7%	72.3*
1.79	2863	521	539	96.7%	138.1%	138.5%	2835	1.20	151.6%	61.8*
total	71817	10945	11200	97.7%	14.3%	15.0%	71152	7.19	15.3%	99.5*

Tabela 11 - Cristal de lisozima em tampão TRIS-HCl (pH 8.0) sem filme (controle, experimento nº 66)

RESOLUTION	NUMBER OF REFLECTIONS			COMPLETENESS	R-FACTOR					
LIMIT	Observed	Unique	Possible	(%)	Observed	Expected	COMPARED	I/SIGMA	R-meas	CC(1/2)
4.13	6364	1001	1007	99.4%	3.3%	3.8%	6360	47.25	3.5%	99.9*
3.27	6048	951	957	99.4%	3.5%	4.0%	6044	44.18	3.8%	99.9*
2.86	6035	923	925	99.8%	3.8%	4.3%	6032	39.50	4.1%	99.9*
2.60	5972	900	905	99.4%	4.2%	4.7%	5968	35.71	4.6%	99.8*
2.41	5781	925	927	99.8%	4.5%	4.9%	5780	32.35	4.9%	99.7*
2.27	5943	891	894	99.7%	4.9%	5.2%	5942	31.15	5.3%	99.6*
2.16	5506	853	856	99.6%	5.0%	5.4%	5506	28.66	5.4%	99.8*
2.06	6102	964	964	100.0%	5.7%	5.8%	6101	25.91	6.2%	99.8*
1.98	6057	912	915	99.7%	6.5%	6.5%	6053	24.05	7.1%	99.7*
1.92	5083	771	773	99.7%	7.0%	7.0%	5081	22.45	7.6%	99.7*
1.86	5128	895	898	99.7%	7.1%	7.0%	5121	20.81	7.8%	99.7*
1.80	5371	991	997	99.4%	7.8%	7.9%	5363	18.43	8.6%	99.6*
1.75	4599	926	941	98.4%	8.4%	8.4%	4575	16.29	9.3%	99.4*
1.71	3638	837	845	99.1%	8.6%	9.2%	3607	14.55	9.8%	99.3*
1.67	3918	889	907	98.0%	8.7%	9.1%	3888	14.55	9.8%	99.3*
1.64	2963	704	746	94.4%	10.6%	10.3%	2934	12.86	12.1%	98.4*
1.60	3508	974	1075	90.6%	9.7%	10.3%	3409	10.71	11.3%	98.6*
1.57	2460	781	901	86.7%	9.6%	10.8%	2295	9.44	11.2%	98.6*
1.55	1464	495	626	79.1%	9.8%	10.2%	1320	9.02	11.4%	97.8*
1.52	1691	623	1001	62.2%	10.2%	10.9%	1446	8.05	12.0%	97.8*
total	93631	17206	18060	95.3%	4.1%	4.6%	92825	24.28	4.5%	99.9*

Tabela 12 - Cristal de lisozima em tampão TRIS-HCl (pH 8.0) utilizando filme de lisozima em tampão fosfato (experimento nº 74)

RESOLUTION	NUMBER OF REFLECTIONS			COMPLETENESS	R-FACTOR					
LIMIT	Observed	Unique	Possible	(%)	Observed	Expected	COMPARED	I/SIGMA	R-meas	CC(1/2)
4.53	4884	776	781	99.4%	5.5%	5.9%	4879	28.73	5.9%	99.6*
3.60	4960	710	710	100.0%	5.8%	6.3%	4958	28.77	6.2%	99.6*
3.14	4492	713	716	99.6%	5.9%	6.3%	4490	26.63	6.5%	99.5*
2.86	4593	681	682	99.9%	6.4%	6.7%	4590	24.59	6.9%	99.6*
2.65	4825	701	701	100.0%	6.8%	7.3%	4823	22.00	7.3%	99.5*
2.49	4453	707	711	99.4%	7.2%	7.7%	4447	19.74	7.8%	99.6*
2.37	4386	650	651	99.8%	8.4%	8.6%	4383	17.86	9.0%	99.4*
2.27	4523	662	663	99.8%	8.6%	8.9%	4520	17.26	9.3%	99.5*
2.18	4591	693	693	100.0%	10.0%	10.2%	4591	14.83	10.8%	99.3*
2.10	4561	731	734	99.6%	11.7%	11.7%	4555	12.54	12.8%	98.6*
2.04	4088	607	610	99.5%	13.6%	13.4%	4087	11.63	14.7%	99.0*

1.98	4803	697	698	99.9%	15.6%	15.5%	4801	10.49	16.8%	98.5*
1.93	4263	641	643	99.7%	17.2%	17.5%	4258	9.20	18.7%	98.7*
1.88	4242	692	706	98.0%	20.2%	19.5%	4229	8.04	22.0%	97.8*
1.84	3478	597	622	96.0%	25.8%	26.4%	3468	6.16	28.2%	96.2*
1.80	3723	663	697	95.1%	27.0%	27.0%	3704	5.82	29.6%	96.3*
1.76	3811	709	749	94.7%	30.9%	30.9%	3784	4.92	34.0%	95.3*
1.73	2683	561	597	94.0%	37.5%	39.4%	2661	3.92	42.0%	88.1*
1.70	2795	615	651	94.5%	42.0%	42.4%	2758	3.53	47.1%	87.6*
1.67	2985	643	696	92.4%	45.9%	46.3%	2940	3.24	51.1%	86.3*
total	83139	13449	13711	98.1%	7.3%	7.7%	82926	14.40	7.9%	99.7*

Tabela 13 - Cristal de lisozima em tampão TRIS-HCl (pH 8.0) utilizando filme de lisozima em tampão TRIS-HCl (experimento nº 76)

RESOLUTION	NUMBER OF REFLECTIONS			COMPLETENESS	R-FACTOR					
LIMIT	Observed	Unique	Possible	(%)	Observed	Expected	COMPARED	I/SIGMA	R-meas	CC(1/2)
4.53	2867	766	781	98.1%	1.9%	2.1%	2817	56.87	2.2%	99.9*
3.60	2972	706	710	99.4%	1.9%	2.2%	2960	59.35	2.2%	99.9*
3.14	2752	710	716	99.2%	2.0%	2.3%	2707	53.71	2.4%	99.9*
2.86	2824	678	682	99.4%	2.6%	2.6%	2799	47.11	3.0%	99.8*
2.65	2945	693	701	98.9%	2.7%	2.9%	2925	41.28	3.1%	99.9*
2.49	2746	693	711	97.5%	2.9%	3.0%	2714	37.89	3.4%	99.9*
2.37	2718	642	651	98.6%	3.4%	3.4%	2706	35.70	3.9%	99.8*
2.27	2830	653	663	98.5%	3.5%	3.5%	2813	33.94	4.0%	99.8*
2.18	2679	690	693	99.6%	3.7%	3.7%	2649	30.09	4.3%	99.8*
2.10	2956	715	734	97.4%	4.3%	4.3%	2928	27.36	4.9%	99.7*
2.04	2629	610	610	100.0%	4.8%	4.7%	2616	25.38	5.5%	99.8*
1.98	2901	672	698	96.3%	5.8%	5.7%	2879	22.18	6.6%	99.6*
1.93	2558	633	643	98.4%	5.6%	5.8%	2531	20.33	6.5%	99.7*
1.88	2487	642	706	90.9%	6.6%	6.6%	2451	18.02	7.6%	99.5*
1.84	2136	583	622	93.7%	8.1%	8.1%	2109	14.37	9.5%	99.0*
1.80	2214	616	697	88.4%	9.1%	8.9%	2173	12.93	10.6%	98.8*
1.76	2086	676	749	90.3%	9.1%	9.2%	1989	11.04	10.8%	99.0*
1.73	1667	513	597	85.9%	11.4%	11.5%	1615	9.74	13.5%	97.9*
1.70	1799	569	651	87.4%	12.0%	12.1%	1747	9.00	14.4%	97.4*
1.67	1798	587	696	84.3%	13.0%	12.9%	1739	8.25	15.5%	97.3*
total	50564	13047	13711	95.2%	2.7%	2.9%	49867	29.85	3.2%	99.9*

Tabela 14 - Cristal de lisozima em tampão TRIS-HCl (pH 8.0) utilizando filme de lisozima em tampão fosfato (experimento nº 80)

RESOLUTION	NUMBER OF REFLECTIONS			COMPLETENESS	R-FACTOR					
LIMIT	Observed	Unique	Possible	(%)	Observed	Expected	COMPARED	I/SIGMA	R-meas	CC(1/2)
5.59	2705	407	429	94.9%	6.4%	7.2%	2689	21.15	6.9%	99.5*
4.44	2474	385	401	96.0%	8.7%	9.5%	2456	15.42	9.5%	99.4*
3.88	2464	363	381	95.3%	9.0%	10.0%	2453	14.95	9.8%	98.9*
3.52	2477	372	386	96.4%	11.2%	11.8%	2467	13.07	12.1%	99.3*
3.27	2122	347	367	94.6%	15.6%	15.8%	2109	9.55	17.2%	98.3*

3.08	2375	350	360	97.2%	18.4%	18.3%	2371	9.73	20.1%	98.0*
2.92	2654	388	396	98.0%	24.4%	27.0%	2644	6.92	26.6%	97.6*
2.80	2059	328	342	95.9%	34.0%	31.6%	2052	5.67	37.2%	96.0*
2.69	2457	365	378	96.6%	39.4%	38.0%	2452	5.15	43.0%	95.8*
2.60	2346	350	354	98.9%	41.7%	44.9%	2341	4.70	45.4%	92.2*
2.51	2538	407	410	99.3%	46.7%	46.7%	2532	4.36	51.2%	91.4*
2.44	2317	343	349	98.3%	59.2%	58.9%	2313	3.59	64.2%	90.4*
2.38	2300	343	344	99.7%	64.7%	65.5%	2299	3.34	70.3%	89.4*
2.32	2614	372	375	99.2%	58.3%	59.4%	2613	3.72	63.1%	89.0*
2.27	2334	335	343	97.7%	85.6%	85.6%	2330	2.66	92.8%	89.4*
2.22	2582	374	379	98.7%	86.0%	88.5%	2579	2.43	93.2%	87.2*
2.17	2490	398	402	99.0%	134.5%	129.5%	2481	1.66	146.8%	71.6*
2.13	2257	352	356	98.9%	150.6%	150.5%	2246	1.44	163.9%	78.9*
2.10	1701	285	290	98.3%	211.6%	211.5%	1693	0.98	232.9%	60.2*
2.06	1124	336	393	85.5%	104.7%	103.8%	1074	1.23	123.1%	54.7*
total	46390	7200	7435	96.8%	17.9%	18.5%	46194	6.78	19.5%	99.2*

Tabela 15 - Cristal de lisozima em tampão TRIS-HCl (pH 8.0) utilizando filme de lisozima em tampão TRIS-HCl (experimento nº 82)

RESOLUTION	NUMBER OF REFLECTIONS			COMPLETENESS	R-FACTOR					
LIMIT	Observed	Unique	Possible	(%)	Observed	Expected	COMPARED	I/SIGMA	R-meas	CC(1/2)
5.10	3364	518	556	93.2%	3.4%	3.5%	3280	41.39	3.6%	99.9*
4.05	3359	495	512	96.7%	3.4%	3.7%	3308	40.36	3.7%	99.9*
3.54	3373	479	500	95.8%	4.4%	4.6%	3327	33.14	4.7%	99.9*
3.21	3065	486	505	96.2%	5.7%	5.8%	3012	25.31	6.1%	99.7*
2.98	3261	468	486	96.3%	8.3%	8.5%	3230	18.96	8.9%	99.6*
2.81	3191	455	472	96.4%	12.0%	12.2%	3169	13.84	12.9%	99.2*
2.67	3450	471	487	96.7%	14.3%	14.5%	3429	11.60	15.3%	98.9*
2.55	3109	480	493	97.4%	17.5%	17.6%	3081	9.54	18.9%	97.8*
2.45	3120	478	489	97.8%	26.1%	25.5%	3091	6.91	28.2%	96.6*
2.37	3044	440	452	97.3%	28.3%	29.1%	3015	6.05	30.3%	95.7*
2.29	3487	505	513	98.4%	27.7%	27.4%	3454	6.26	29.7%	95.9*
2.23	3120	440	449	98.0%	32.9%	32.9%	3096	5.17	35.3%	96.3*
2.17	3024	475	482	98.5%	45.1%	44.3%	3000	3.74	48.6%	91.5*
2.12	2816	446	452	98.7%	48.6%	47.6%	2790	3.50	52.6%	92.4*
2.07	3218	488	499	97.8%	51.1%	51.0%	3188	3.10	55.0%	89.7*
2.03	2770	413	421	98.1%	74.4%	75.5%	2742	2.23	80.0%	81.6*
1.98	4023	578	582	99.3%	63.8%	64.4%	3984	2.60	68.4%	86.5*
1.95	2523	371	373	99.5%	95.0%	95.5%	2500	1.72	101.9%	76.6*
1.91	3534	537	541	99.3%	101.0%	100.7%	3505	1.63	108.9%	76.7*
1.88	1675	297	435	68.3%	122.6%	124.1%	1635	1.25	133.8%	63.7*
total	62526	9320	9699	96.1%	10.0%	10.1%	61836	12.38	10.7%	99.8*